Biointerface Research in Applied Chemistry
Open-Access Journal (ISSN: 2069-5837)

Review
Volume 15, Issue 2, 2025, 21
https://doi.org/10.33263/BRIAC152.021

Nano MgO: A Promising Biocompatible Candidate in the Modern Medicinal Field

Bapu R. Thorat [1,*], Devidas S. Bhagat [2,*], Vilas A. Chavan [2,3], Swati Wavhal [4]

[1] Department of Chemistry, Government Arts and Science College, MS, Chhatrapati Sambhajinagar, 431 001. India; bthorat78@gmail.com
[2] Department of Forensic Chemistry and Toxicology, Government Institute of Forensic Science, Chhatrapati Sambhajinagar - 431 004, MS, India; devidas.bhagat@gov.in
[3] Aditya University, Aditya Nagar, ADB Road, Surampalam, East Godawari District, 533 437, Andhra Pradesh, India; vilas.chavan47@gmail.com
[4] Government of Maharashtra's, Ismail Yusuf College of Arts, Commerce, and Science, Mumbai 400 060, (MS), India; swavhal@gmail.com
* Correspondence: devidas.bhagat@mah.gov.in (D.S.B.)
Scopus Author ID 57327243700
Received: 3.06.2024; Accepted: 5.01.2025; Published: 12.04.2025

Abstract: Magnesium oxide (MgO) nanoparticles have been created using simple chemical and environmentally sustainable methods, with magnesium chloride, magnesium acetate, and magnesium nitrate as catalysts. The surface area, crystal morphology, and reaction sites change with synthesis conditions. MgO nanocomposite or drug delivery nanocomposite are prepared for active drugs with various biological functions like antibacterial, anti-cancer, anti-inflammatory, bone repairing mechanism, anti-diabetics, cytotoxicity, etc. Because of their high strength-to-weight ratio and good biocompatibility in acidic media, nano-MgO composites are used in bone implants, biodegradable fibers, and screws. Nano MgO has optimum biocompatibility due to its less toxic nature. It is also used with other nanocomposites, and its physicochemical properties change with the doping of other metals or metal oxides.

Keywords: nano-MgO; MgO-composites; antimicrobial; anti-cancer; bone implant.

1. Introduction

A nanoparticle of 0 - 100 nm size exhibits properties different from bulk materials in various structures. Its shapes include spiral, flat, conical, hollow, nano-belts, spherical, nano-rods, nanotubes, etc. These nanoparticles play an important role in synthesis as catalysts, improving physicochemical characteristics, the medicinal field, atmospheric pollution prevention, wastewater treatment, soil sediments, additives, and so on [1].

Numerous methods have been reported for synthesizing nanomaterials, which vary depending on the nanomaterial and its properties. Physical, chemical, green, and microwave-assisted synthesis were common methods [2]. However, in some physical and chemical syntheses, toxic materials that showed some adverse effects were eliminated by excellent alternative eco-friendly methods [3], such as green or biological methods [4]. The use of microbes (bacteria, fungi, algae, and such), enzymes, plants, and plant extracts in the greener synthesis of nanoparticles is known as the biosynthesis of nanoparticles [5]. The silver and gold nanomaterials were synthesized by using microorganisms [6]. Other common methods for

nanomaterial synthesis, like the sol-gel method, co-precipitation, hydrothermal, and so on, have been reported [7]. Green synthesis, hydrothermal, sol-gel, precipitation, and microwave-assisted methodologies were also used to synthesize nano-MgO [8]. Different conventional and MW methods for the preparation of nano MgO are depicted in figure 1. These techniques were most frequently used because they are safe, fast, less time-consuming, and non-toxic methods [7, 8]. The greener method used magnesium nitrate as an Mg source and *Nephelium lappaccum peel* as a natural source; no other chemicals were used directly to prepare nano-MgO.

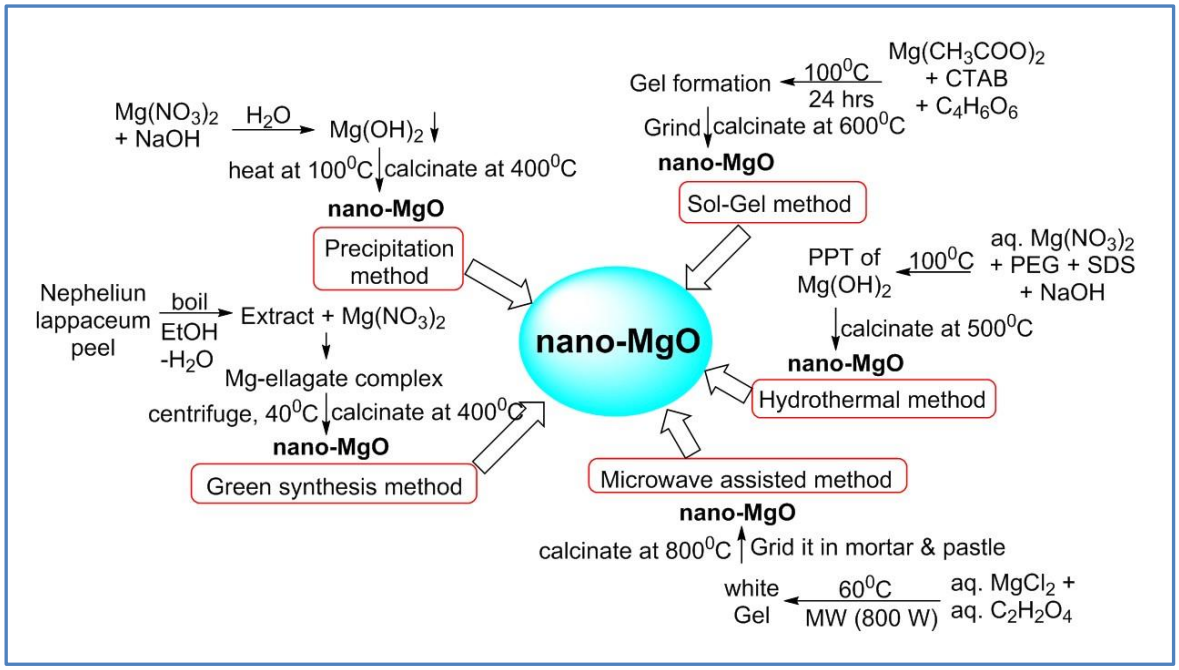

Figure 1. Different conventional and MW methods for the preparation of nano MgO.

Magnesium cation is the second-most prevalent intracellular constituent and the fourth most abundant overall in the human body [9]. It is also a cofactor for more than 300 enzymes [10]. Nearly 7-11% of hospitalized patients have magnesium deficiency problems. It is one of the factors associated with most critical health issues and disorders, such as diabetes, hypertension, colon cancer, sudden cardiac death, coronary heart disease, osteoporosis, etc. In most cases, magnesium oxide or magnesium salts such as magnesium sulfate ($MgSO_4$) are administered to patients via intravenous or intramuscular injection to treat symptomatic magnesium deficiency [11]. However, excessive magnesium administration causes hypermagnesemia, particularly in patients with impaired renal function. Hypermagnesemia can cause a variety of health problems, such as neuromuscular disorders, cardiac arrest, hypertension, and hypocalcemia [12].

There are several medicinal applications of nano-MgO particles; some are listed in figure 2. These reported MgO applications could be attributed to relatively high surface areas and crystal morphological traits with more reactive sites on the surface [13].

One significant research found that high concentrations of Magnesium oxide nanoparticles (250 and 500 µg. mL^{-1}) injected into rats significantly increased hemoglobin, RBCs, WBCs, and hematocrit compared to the control group ($P < 0.05$). The findings also demonstrate that nano-MgO particles increased the levels of alkaline phosphatase and aspartate aminotransferase while not affecting the levels of gamma-glutamyl transpeptidase, alanine aminotransferase, urea, and creatinine when compared with the control group ($P < 0.05$). A histopathological examination of the rat liver revealed proliferation of bile ductules, congestion

in some areas of the liver sinusoids, and apoptotic cells in high-dose groups, but no histopathological changes in kidney functions. At last, it was determined that magnesium nanomaterials at concentrations less than 250 µg mL^{-1} are reliable for use in the desired applications [14].

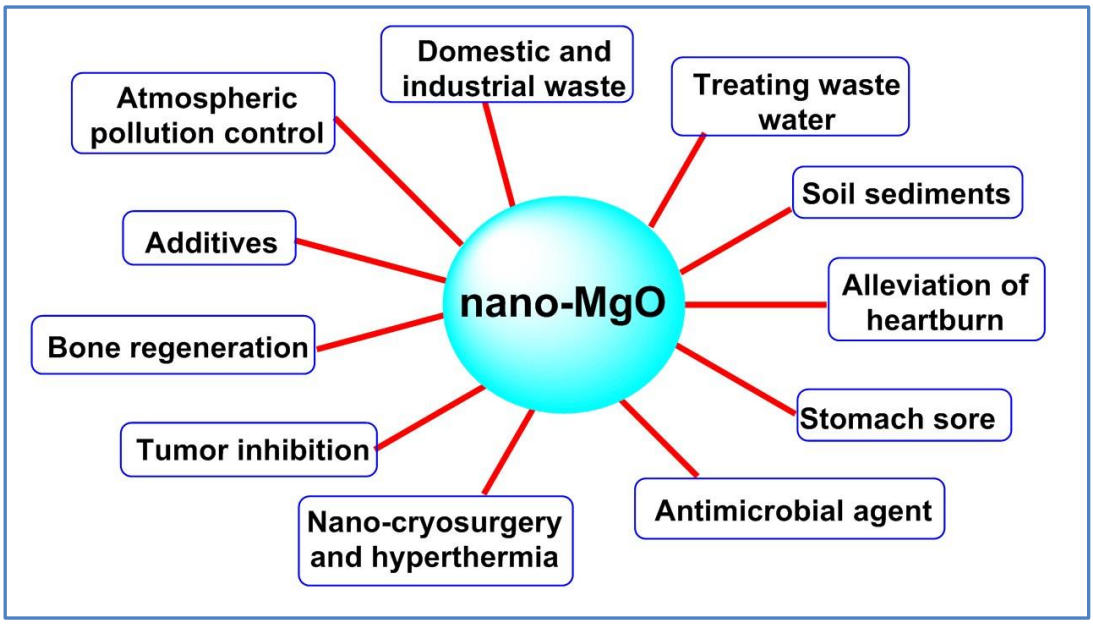

Figure 2. Medicinal importance of nano-MgO.

2. Medicinal Application of Nano MgO

Several contagious diseases have been reported to cause millions of deaths worldwide each year. Following the discovery of antibiotics in the twentieth century, there was a tremendous improvement in the medical sector and a reduction in the deaths and illnesses caused by such infectious diseases. However, as time passes, modernization of society, changes in environmental conditions, population growth, dramatic changes in lifestyle and food, and evaluation of microorganisms all contribute to either impedance in microorganisms or the development of new diseases [15].

2.1. Bactericidal activity/anti-infectious diseases.

As a result, current antibiotics and chemotherapeutics are ineffective against evolved microorganisms, necessitating the development of new antibiotics, the search for new drugs, or chemical modifications to existing drugs. The period and effectiveness of new drugs against microbial pathogens are issues for drug development. It does not guarantee that microbial pathogens will not create drug resistance in the future. As a result, it is critical to develop more impactful and long-term solutions to such infections [16].

The existing antibiotics and chemotherapeutic agents killed the microbes or interfered with their growth. Several antibiotics are used for the treatment, from penicillin in the late 1940s to topical antibiotic ointments (such as Neosporin) to intravenously injected antibiotic solutions. Examples: vancomycin, β-lactam drug, bacitracin (inhibiting cell wall synthesis); tetracyclines, aminoglycosides, chloramphenicol, macrolides (inhibiting protein synthesis); rifampicin and fluoroquinolones (inhibits nucleic acid synthesis); trimethoprim and sulfonamides (inhibits the metabolic pathways); and polymixin B (interfering in the membrane integrity) [17].

Along with several other causes of the use of antibiotics, insufficient drug delivery at the infection site is one of the major limitations of conventional therapy that increases the cost of treatment, period, problems of poor uptake, and may lead to harmful side effects to the host. Today, more than 75% of microorganisms have developed resistance to at least one of the most commonly used medicines or drugs for treatment. The microbial pathogens developed resistance by altering the drug target, developing alternative metabolic pathways for the growth, inactivating the target enzymes, or inhibiting efflux transport. Some pathogens that can be treated only with potentially toxic drugs or a combination of drugs were detected. Some important drugs/antibiotics, along with resistant bacteria and their mechanism, are shown in Table 1.

Table 1. Drug/antibiotics, drug-resistant bacteria, and their resistance mechanism [18].

Drug	Microorganism	Mechanism of resistance
Quinolone	*Gonococci*	Mutation in target
Vancomycin	*Enterococcus*	Changes in target
Sulfonamide	*Enterococcus*	Overproduction of the target site, Development of alternate growth requirement
β-lactam (carbapenem)	*Enterobacteriaceae (e.g.: E. coli)*	Drug degrading enzyme
Macrolide	*Streptococcus pneumoniae*	Drug efflux pump, active efflux
Multiple drugs	*Pseudomonas aeruginosa*	Multiple factors, including loss of porin, drug efflux pump, and drug-modifying enzyme
β-lactam (methicillin)	*Staphylococcus aureus*	Production of an additional enzyme that avoids binding
Vancomycin	*Staphylococcus aureus*	Cell wall thickening changes in the target

Compared to conventional therapy, nanostructured antimicrobial agents or nanosized drug carriers were helped to eliminate the resistance, reduce the toxicity, improve the pharmacokinetics & therapeutics of the drug, and, therefore, the cost of the treatment. Nanoparticles of metal oxides and metals were found to possess good antimicrobial activity, and the pathogens did not develop resistance against them. The mechanism of action of such nanoparticles against microbial pathogens is as follows: they directly disrupt the cell wall or inhibit DNA/protein/enzyme synthesis, or they generate free radicals, i.e., photocatalytic generation of reactive oxygen, which damages cellular and viral components. The targeted delivery of the drug at the point of infection improves biodistribution and drug accumulation in the specific body site. Various metals and metal oxides have been reported to act as nano-antibiotics, with potential applications against infectious diseases. Microorganisms did not develop resistance to them, and nano-metals had no adverse effects on human cells. Examples: Ag-nanoparticle [19], Au-nanoparticles [20], TiO_2-nanoparticles [21], Al_2O_3-nanoparticles [22], Cu, Cu_2O & CuO nanoparticles [23], Fe-oxide nanoparticles [24], MgO-nanoparticles [25], ZnO-nanoparticles [26], etc. The bactericidal activity of metal oxides such as MgO, ZnO, and TiO_2 was primarily due to (i) effortlessly binding of nanomaterials on the bacterial cell membrane and subsequent damage; (ii) easily penetrating the cell and binding to specific targets via surface oxygen and rendering them inactive; and (iii) creation of reactive oxygen species (ROS) on their surface, which automatically increases intracellular oxidative stress. ROS production causes lipid peroxidation in bacteria [27].

However, some nanoparticles show bactericidal activity not mediated by ROS, implying that oxidative stress is not the main mechanism of bacterial cell death [8]. According to the findings, bactericidal activity depends not only on the shapes, sizes, surface characteristics (e.g., hydrophobicity), and composition of the nanomaterials but also on the species of bacteria [28]. Nanoparticles of ZnO, MgO, or CaO are not toxic, and their actions

are not photoinduced like TiO_2. In contrast to other solid bactericidal agents such as backed silver or backed copper, nan-TiO_2, nano-MgO particles have some benefits, such as being non-toxic up to a concentration of 250 µg mL-1 and being easily synthesized from readily available, inexpensive precursors. As a result, nano-MgO can be used as a solid bactericidal material in various applications [29].

Because of anomalies in the structures of nano-MgO particles, reactive oxygen species (ROS) can be produced on the surface [30], which is a remarkable property that attracts interest as a potential antibacterial material: the nano-MgO can easily inactivate or kill bacteria either by the formation of ROS or through adsorption of negatively charged bacteria on their positively charged surfaces.

Microwave irradiation created nano-MgO from magnesium acetate diluted in ethylene glycol. The antibacterial activity of small nanocrystalline MgO against gram-positive *S. aureus* and gram-negative *E. coli* bacteria was tested. The results show that small particles of MgO are more active, and the activity decreases with increasing particle size, indicating that MgO has size-dependent antimicrobial activity against both gram-positive and gram-negative bacterial strains such as *E. coli* and *S. aureus* [31].

Amorphous MgO was found to have no or inactive bactericidal activity against the same microorganism strains. The increased activity of small nano-MgO could be attributed to the formation of active oxygen species that are active both inside the bacterial cell and on the cell wall [32]. As a result, nano-MgO alone or in combination with other ingredients has been proposed for the treatment and preservatives of some food products to enhance microbiological food safety [33].

Nano-MgO was discovered to be safe for mammals as well as the environment. Unfortunately, prolonged exposure to nano-MgO may result in some human and environmental problems. The results of a cytotoxicity and neurotoxicity research of nano-MgO particles on SH-SY5Y cell lines show that nano-MgO particles are not toxic towards both differential and nondifferential SH-SY5Y cells at concentrations ranging from 1nM to 1mM for 24, 48, and 72 hours [34].

ZnMgO nanomaterials of various shapes, such as nanocubes, nanorods, and nano-tetrapods, were created and tested for bactericidal and toxic effects against mammalian cells. These particles were discovered to be more bactericidal, particularly against Gram-positive bacteria, while causing no harm to mammalian cells. Pure nano-ZnO was discovered to be harmful to mammalian cells [35].

Sawai *et al. (1997)*proposed another framework for the antibacterial activity of nano-MgO particles. Moisture absorbs the surface of the nanoparticles, creating a thin water layer around the particles. The pH of the water above the layer may be greater than its equilibrium value in the solution. The higher pH of the nanoparticles' surface could affect the bacteria membrane, causing cell death [36].

Although halogens such as fluorine, chlorine, and bromine have strong bactericidal properties, they are not widely used due to their high toxicity. Metal-halogen complexes are formed by halogens interacting with and suppressing specific cellular enzymes [37]. Mg-halogen nanomaterials destroy the microbial cell envelope and end up causing intracellular content leakage due to rapid peroxidation caused by ROS. Nano-MgO particles have a distinctive capacity to absorb and retain halogens, which increases fivefold in nanomaterials formulations containing nano-MgO. A combined effect of absorbing halogen on nano-MgO enhances bactericidal activity over halogen and converts the halogen to powder form [13].

The bactericidal activity of chloride and bromide in conjunction with nano-MgO was examined against *B. subtilis*, *B. megaterium*, and E. *coli* endospores. MgO-halogen nanomaterials completely killed E. *coli* and *B. megaterium* in 20 minutes, whereas *B. subtillis* has some resistance, and only about 30% of the bacteria are killed. MgO-halogen nanomaterials were discovered to be 68% more effective bactericidal agents than halogen alone.

Some formulations of nano-MgO/nano-CaO and active forms of halogens such as chlorine & bromine in nanoscale were formulated and evaluated for their antimicrobial activities. Antimicrobial tests were performed on these nanocrystalline materials against *Escherichia coli, Bacillus globigii, Bacillus cereus,* aflatoxins, and MS2 bacteriophage [31]. When these composites come into contact with vegetative *Escherichia coli, Bacillus cereus,* or *Bacillus globigii* cells, over 90% are killed within just a few minutes. Bacillus species' spores decontaminate in a matter of hours. All composites were decontaminated in water for several minutes with aflatoxins and MS2 bacteriophage (human enterovirus surrogate).

Magnesium oxide (MgO) nanoparticle-incorporated polycaprolactone (PCL)/gelatin nanofibrous membranes [38] were prepared by electro-spinning and investigated their potential for wound healing of full-thickness skin wounds [39], wound dressing and fighting bacterial infection. This nano-MgO-incorporated membrane is pliable, flexible, and hydrophilic, allowing for convenient interaction with wound beds. The percentage of nano-MgO in the membrane affects its cytocompatibility and bactericidal efficiency: lower amounts promulgated while higher amounts inhibited fibroblast, endothelial cell, and macrophage proliferation. More than 90% of *S. aureus*, 98% of *E. coli*, and 94% of *S. epidermidis* were inhibited by the nano-MgO. The incorporation of nano-MgO particles into the electrospun membranes could be used to prevent wound bacterial infections [40].

Because of their non-toxicity, nano-MgO particles have been used as anti-bacterial agents to enhance food safety. The antibacterial activity of resazurin (a redox-sensitive dye) microplate assay (measuring inhibition of bacterial growth) against *Escherichia coli* O157:H7, *Campylobacter jejuni*, and *Salmonella Enteritidis* was investigated [41]. The MIC values of nano-MgO to 10^4 CFU/ml *Escherichia coli* O157:H7, *Campylobacter jejuni*, and *Salmonella Enteritidis* were 1, 0.5, and 1 mg/ml, respectively. A different study found that after contact with nano-MgO, cell membrane permeability increased. H_2O_2 produced by nanoparticles induces (oxidative stress) the gene expression of KatA, the sole catalase in *C. jejuni* responsible for H_2O_2 decomposition. These practicals attacked the cell membrane and caused oxidative stress in the microbial pathogens, which resulted in death. It was discovered that different compositions of nano-MgO particles significantly inhibited both gram-positive and gram-negative bacterial strains [42].

C. albicans is a significant pathogen that causes many human infectious diseases. Due to multidrug resistance, nonbiodegradability, toxicity, and poor biocompatibility, very few standard treatments are available for treating fungal infections. The antifungal activity of nano-MgO particles, including key virulence factors such as preliminary adhesion, two-phase morphological transformation, and biofilm formation of *C. albicans* fungi strains, was evaluated using the micro-broth dilution method, MTT assay, and fluorescence microscopy [43].

According to the findings, MgO NPs strongly suppressed C. albicans biofilm formation, two-phase morphological transformation, initial adhesion, growth, and metabolic activity. The initial perception is that nano-MgO particles could be used as a viable antifungal drug to prevent the spread of *Candida* infection by coating medical devices with them. A new

polymeric system containing immobilized MgO/CuO composite material and nystatin-loaded MgO/CuO nanostructure in sodium alginate microspheres was developed to deliver the antifungal drug. Microspheres were created using the ionotropic gelation technique and calcium chloride as a cross-linker. These Nys-MgO/CuO NP-encapsulated microspheres are compatible and can be utilized as a sustained, controlled drug release system against MDR pathogenic *C. albicans* at pH 5.5 [44].

Green nano-MgO nanoparticles have been synthesized in the presence of light from an aqueous leaf extract of *Swertia chirayaita* and tested for bactericidal activity against various strains of both gram-positive and gram-negative bacteria using the agar well diffusion method. The size of these crystalline face-centered cubic nanoparticles is <20 nm. These particles were found to be active against the bacterial strains *S. aureus* - MTCC-9442, *S. epidermidis* - MTCC-2639, *B. cereus* - MTCC-9017, *E. coli* - MTCC-9721, *P. vulgaris* - MTCC-7299, and *K. pneumonia* - MTCC-9751 [45].

Green nano-MgO was discovered for the first time in the cell filtrate of the endobacterium *Burkholderia rinojensis*. The antifungal and antibiofilm activities of these particles against Fusarium oxysporum f. sp. lycopersici were impressive [46]. More than a hundred bacterial genus Burkholderia are found in the water, soil, insects, rhizospheres, and arbuscular mycorrhizal fungi [47]. These species were prepared with several secondary metal bodies showing insecticidal, antifungal, antibacterial properties [48].

The nano-MgO concentration of 15 µg/ml severely suppressed the fungus's mycelial growth, whereas the pathogen's biofilm formation was eliminated at 1.92 µg/mL. The nano-MgO induces several morphological changes in biofilm formation and hyphal morphology, significantly damaging the fungal membrane integrity. $Mg(NO_3)_2.6H_2O$ and *Emblica officinalis* fruit extract were also used to create nano-MgO particles with a diameter of nearly 27 nm. This nano-MgO has been treated with cotton fiber, which has been shown to have greater antibacterial activity against *S. aureus* and *E. coli*. Cotton fibers/textures infused with nano-MgO have been used in the medical field for various applications, including surgical clothing, active cotton bandages, wound stressing, bandage bed lining, and other textile materials for medical and food application areas [49].

A nanotextured MgO sheet demonstrated promising antibacterial [50] and tissue regeneration activity, suggesting that it could benefit patient bond implant protection. It has been reported that MgO nanoparticles have the contact-based bactericidal potential of MgO nanoparticles against a wide range of bacteria. Several other nano-MgO samples with structural defects were synthesized, and their hydrolysis kinetics, antibacterial activity against *E. coli* (ATCC 47076), *S. epidermidis*, and *Ps. aeruginosa*, and reactive oxygen species (ROS) generation potential were analyzed [51].

Another study investigated new nanotextured MgO microrod composites embedded in various biodegradable polymer matrixes, including poly-lactide-co-glycolide (PLGA), poly-lactide (PLA), and polycaprolactone (PCL). The PLGA matrix was found to be the most effective of the three. The PLGA/nano-MgO matrix was found to be the most effective bactericidal agent against planktonic *E. coli* or *sessile S. epidermidis*, *S. aureus* (multidrug resistant-MRSA), and three clinical strains isolated from implant-associated infections (*S. aureus, E. coli,* and *Ps. aeruginosa*) without harming red blood cells [52]. Hickey *et al.* investigated the role of nano-MgO particles in poly (l-lactic acid) (PLLA) and hydroxyapatite-PLLA composites for orthopedic tissue engineering applications [53].

MgO nanomaterials were synthesized using a novel triethylamine-based precipitation method, and their bactericidal behavior against Gram-positive *Staphylococcus aureus* and Gram-negative *Escherichia coli* bacteria was tested using microdilution assays. This was used to make nano-MgO with an average size of 120 nm that has an antibacterial effect with MIC values of 250 and 500 ppm for *S. aureus* and *E. coli* strains, respectively. Atomic Force Microscopy was used to detect structural reforms in bacterial cells, such as membrane collapse, surface changes such as vesicular formation, and changes in longitudinal and horizontal sizes as well as circumference caused by reactive oxygen species (ROS) such as superoxide anion radicals or hydrogen peroxide (H_2O_2) generated on the surface of MgO nanoparticles [54].

A MgO-hydroxyapatite-poly-L-lactic acid (PLLA) nanofiber has been demonstrated to enhance osteoblast adhesion and proliferation in bone tissue engineering. The conventional method of coating nanocrystals demonstrates no decline in bacterial colonization witnessed on the MgO-HA-PLLA nanomaterials. This lower or absence of bactericidal activity could be attributed to the MgO NPs' limited exposure at the surface of the MgO-PLLA nanomaterials. However, it has been reported that direct contact between nano-MgO particles and the bacterial cell membrane is required to cause cell death [55].

As a result, electrophoretic deposition of nano-MgO was reported to result in great exposure of nano-MgO on the substrate's surface. Bacterial infections of implanted artificial materials are a serious healthcare issue that raises costs and harms healthcare practices. Nano-MgO particles have been reported as a promising material for controlling or avoiding bacterial infection and improving or sustaining bone cell functions. Nano-MgO particles electrophoretically accumulated onto poly-L-lactic acid (PLLA) sheets and were identified for the bone implant. Bactericidal testing against *Staphylococcus epidermidis*, *Staphylococcus aureus*, and *Pseudomonas aeruginosa* reveals that as applied voltage increases throughout surface coating electro-deposition, bactericidal activity increases by up to 90% against all three strains. *S. aureus* cells that did attach to high-voltage-prepared nano-MgO-coated PLLA sheets showed classic signs of membrane damage and cell death. The voltage used for coating has an impact on other activities. For example, high-voltage deposition enhances osteoblast adhesion while decreasing fibroblast adhesion. According to additional research, high voltages as high as 120-150 V used for nano-MgO coatings can enhance bone cell attachment, reduce fibrous capsule formation, and resist bacterial colonization [56].

Mg and its alloys have been employed in biomedical devices for musculoskeletal injury repair because they exhibit appealing biological and mechanical properties and are biodegradable. In the fixation of rabbit femoral intercondylar fractures [57], bone formation for the fixation of femoral neck fractures in goats [58], and vascularized bone grafts for human patients [59], the implant screw is made of high purity Mg (99.99% pure). However, their rapid degradation in physiological fluids restricted their clinical translation because it led to the formation of hydrogen gas and the quick discharge of HO^-, which could negatively affect the healing process. Internally implanted devices become infected due to biofilm formation, which prevents host cell attachment to the implants and thus interferes with osseointegration, resulting in implant failure. An Mg/nano-MgO fabrication demonstrated bactericidal activity against *S. aureus*. As a result, this formation was employed in clinical trials for antimicrobial biodegradable implants [60].

Bacterial wilt is a severe infection that affects many food crops. Some biotic or abiotic stress treatments result in the cellular generation of reactive oxygen species (e.g., superoxide radicals, hydrogen peroxide (H_2O_2), and hydroxyl radicals), which may significantly boost

resistance to bacterial infections [61]. A root of tomato plants was cultured with *R. solanacearum* and then treated with nano-MgO particles; however, the inhibition of bacterial wilt was noticeable if the roots were soaked with a nano-MgO particle liquid before inoculation with the pathogen. This could be due to the rapid formation of reactive oxygen species (ROS) due to the reaction between nano-MgO and polyphenols found in tomato plant roots. Furthermore, histochemical analyses of the MgO NP-treated plant show that β-1,3-glucanase and tyloses accumulated in the xylem and apoplast of hypocotyl pith tissues. Plant hormones such as Jasmonic acid-inducible LoxA, systemic resistance-related GluA, ethylene-inducible Osm, and salicylic acid-inducible PR1 (which plays a crucial role in defense responses as signaling molecules) [62] were up-regulated in both the roots and hypocotyls of tomato plants after MgO NP intervention. In general, nano-MgO causes systematic resistance to *R. solanacearum* in tomato plants [63].

For the first time, nano-MgO particles were tested for fungicidal activity against two soilborne pathogens, *Phytophthora nicotianae* and *Thielaviopsis basicola,* in a greenhouse setting. Nano-MgO can more effectively prevent fungal growth, sporangium formation, spore germination, and sporangium development. After absorption, nano-MgO interacts with fungal cells, causing cell morphological changes or oxidative stress, as observed by SEM and TEM. Compared to untreated controls or nano-MgO, a 500 µg/ml dose of nano-MgO suppressed fungal invasion via root irrigation. A nano-MgO treatment could effectively prevent various fungal infections in agricultural fields [64].

Bacterial brown stripe, caused by the *Acidovorax oryzae* bacterial strain, is a well-known rice disease. It destroyed rice cultivation. S.O. Ogunyemi *et al.* synthesized nano-MgO from *Matricaria chamomilla* L. and studied their inhibition activity against *Acidovorax oryzae* bacterial strain. The findings demonstrate that both nano-MgO samples strongly inhibited the growth of *Acidovorax oryzae* bacteria [65]. MgO nano-flowers were created using commonly available MgO and *Rosmarinus officinalis* L. extracts. Nano-MgO flowers severely hinder biofilm formation, bacterial growth, and motility of *Xanthomonas oryzae pv. oryzae*, the causative agent of rice bacterial blight disease [66]. A new aqua-dispersed composite of nano-MgO particles and sepiolite is prepared and tested for antifungal activity against various phytopathogenic fungi of rice, including *F. verticillioides, B. oryzae,* and *F. fujikuroi*. With ED90 > 230 and 249 µg/mL, respectively, against the test fungi, SE-MgO nanomaterials were a greater fungicide than aqMgO-NPs. Both the SE-MgO nanostructured materials have been recognized as safe by international agencies. Thus, their composite can be a feasible, environmentally benign, efficacious, eco-friendly, and dust strategy for combating fungal threats against phytopathogens [67].

An *in-vitro* and *in-vivo* bactericidal assessment of nano-MgO against *Ralstonia solanacearum* is the causative agent of the catastrophic bacterial wilt affecting tobacco yield. The bactericidal effect of nano-MgO was concentration-dependent [68]. The photoelectrical and antimicrobial properties of green nano-MgO, Ag, and Ag/MgO-nanocomposites prepared from *Aloe Vera* leaf extracts were studied [69]. Under light irradiation, acid-treated nano-MgO [70] and Ag-doped Ag-MgO nanoparticles demonstrated antibacterial activities against E. coli bacteria in 25 minutes. Using a film contact test, different samples of composite resins containing variable mass ratios (0%, 1%, 2%, 4%, 8%) of nano-MgO particles were prepared, and their antimicrobial effects against *Streptococcus mutans* (*S. mutans*) were assessed [71].

Simple air calcination was used to create Fe-doped MgO nanoparticles (NPs). The Fe doping increases oxygen vacancies and OA content (from 13.5% to 41.3%) on the MgO

surface, which may increase the generation of reactive oxygen species (ROS) and, ultimately, the death of *E. coli* (ATCC 25922) [72]. Another study successfully doped Li, Ca, Zn, Ti, Cu, and Ag elements into nano-MgO using either direct one-pot synthesis or post-treatment methods [73]. Compared to other nano-MgO materials and pure nano-MgO, Ag and Cu-doped nano-MgO exhibits superior antibacterial activity and toxicity [74]. The sol-gel method created divalent transition metal ions such as Ni, Co, and Fe with variable contents of 0, 0.01, 0.03, 0.05, and 0.07. The lack of oxygen on the surface of nano-MgO rises as the quantity of dopant ions increases, resulting in enhanced magnetic and bactericidal activity against *E. coli* and *S. aureus*. This study suggests that nanomaterials could be used in place of traditional antibiotics to treat infections resulting from bacterial infections [75].

The antibacterial effect of revised resin rises as the percentage of nano-MgO rises, reaching a maximum of 99.4% when the mass ratio of nano-MgO is 8%. Still, the overall strength of the material declines as the percentage of nano-MgO particles rises. Nano-MgO particles (up to 68.08 nm) were synthesized using a photo-irradiation technique from magnesium acetate, and *A. tricolor* leaf extract usually contains light-sensitive phytochemicals [76].

The fatal dose of nano-MgO against *E. coli* and *S. aureus* was 0.6 ml and 0.4 ml, respectively. In contrast, the fatal dose of traditionally synthesized nano-MgO against both strains of bacteria was 0.4 ml. Green nano-MgO particles were also synthesized from magnesium nitrate and aqueous extract of *P. marsupium* heartwood and tested for antimicrobial, antioxidant, anti-diabetic, and anti-inflammatory activity [77]. These spherical nanostructures with hydroxyl, carboxyl, and phenolic groups function as reducing, stabilizing, or capping agents. These particles are more effective against Gram-positive bacteria like *S. aureus* and *E. coli* (Gram-negative bacteria). These particles are also highly antioxidant, anti-diabetic, and anti-inflammatory.

Biogenic synthesis was used to create nano-MgO nanoflakes (average size 11 nm) from magnesium chloride, *Bauhinia purpurea* leaf extract, and sodium hydroxide. Various phytochemicals, including antioxidants, phenolics, and flavonoids, contribute to the properties of nano-MgO particles. At dose size (250 g/ml), nano-MgO nanoflakes show potential bactericidal activity against *S. aureus* [78]. At pH 8 and 35°C, a *Rhizopus oryaze* fungal strain was employed as a biocatalyst to produce eco-friendly nano-MgO particles (average size of 20.38 ± 9.9 nm). At 200 µg mL^{-1}, these biogenic MgO-NPs exhibit excellent antimicrobial activity against pathogens such as *E. coli*, *Staphylococcus aureus*, *Pseudomonas aeruginosa*, *Bacillus subtilis*, and *Candida albicans*. Fewer MgO-NPs were required to have larvicidal and adult-repellent activity against *Culex pipiens* [79].

The metabolites isolated by *Penicillium chrysogenum* were used to produce a new specimen of biogenic nano-MgO particles (sizes ranging from 7 to 40 nm). At 200 µg mL^{-1}, this sample demonstrated good antimicrobial activity against pathogenic organisms *Escherichia coli*, *Staphylococcus aureus*, *Pseudomonas aeruginosa*, *Bacillus subtilis*, and *Candida albicans*. This activity was proportional to the amount of nano-MgO present. The biogenic nano-MgO particles have high efficacy against *Anopheles stephensi* larvae instars and pupa, with LC50 values of 12.5-15.5 ppm for I.-IV larvae instars and 16.5 ppm for the pupa. Within 150 minutes, 5 mg/cm^2 of MgO-NPs provides 100% protection against adults of *Anopheles stephensi* [80].

Brown algae metabolites, *Cystoseira crinita*, were employed as a biocatalyst in the preparatory work of green nano-MgO particles (sizes of 3–18 nm). It has encouraging

antimicrobial properties against Gram-positive and Gram-negative bacteria and *Candida albicans*, with MIC values ranging from 12.5 to 50 μg mL^{-1}. It has anticancer properties against cancer cell lines (Caco-2) with an IC50 value of 113.4 μg mL^{-1}, whereas it has anticancer activity against normal cell lines (Vero cell) with an IC50 value of 141.2 μg mL^{-1}. It is effective against *Musca domestica* in terms of larvicidal and pupicidal activity. At 10 μg mL^{-1} MgO-NPs, the highest fatality percentages were 99.0%, 95.0%, 92.2%, and 81.0% for *M. domestica* I, II, and III instar larvae and pupa, with LC50 values (3.08, 3.49, and 4.46 μg mL^{-1}) and LC90 values (7.46, 8.89, and 10.43 μg mL^{-1}), respectively. MgO-NPs repelled adults of *M. domestica* at 10 μg mL^{-1} with 63.0%, 77.9%, 84.9%, and 96.8% after 12, 24, 48, and 72 hours, respectively [81].

2.2. Genotoxicity activity.

Nano-MgO particles have unique properties, higher chemical stability, and extensive applications. Despite this uniqueness in the properties and applications, there is still limited knowledge about the human health impact and safety profile. *In-vitro* acute toxicity and genotoxicity of MgO-microparticles (~12 μm) and MgO-nanoparticles (~53 nm) were assessed/studied using Comet assay by introducing orally in female albino Wistar rats. The experiment was conducted using different dosages of these particles (100, 500, and 1000 mg/kg). At different sampling times (24 h and 72 h), rats' whole blood was drawn from the animals' retro-orbital plexus, and liver tissues were separated after sacrifice. The alkaline comet assay was used to examine the isolated liver cells and peripheral blood lymphocytes. Both assays demonstrate a significant increase in % tail DNA at 1000 mg/kg doses of nano-MgO particles at the 24 h and 72 h sampling times. At 500 mg/kg, nano-MgO particles induced a significant percentage of tail DNA at both sampling times in liver cells but only at the 24-hour sampling time in PBL. The administration of nano-MgO particles caused no substantial damage in any of the doses tested. Furthermore, a gradual decrease in the percentage of tail DNA was witnessed over time, which was believed to be due to the processes involved in the intricate DNA repair. According to the findings of this study, particle size plays a crucial role in the induction of toxicity, as nanomaterials induced greater genotoxicity than microparticles [82].

2.3. Cytotoxic effect (anti-cancer activity).

Nano-MgO particles were found to be a potential bactericidal and fungicidal agent against different pathogens. Due to non-bio toxicity, nano-MgO particles are potential candidates in drug discovery, hyperthermia systems, and MRI [83]. MgO-nanoparticles attach to HSA molecules (proteins that contribute to creating the protein corona on the NP's surface) via hydrophobic interactions, causing minor secondary structural changes in HSA. The nano-MgO particles also exhibit selective cytotoxicity against human leukemia cell lines (K562 cell line) (by MTT assay). At the same time, no adverse effect was observed on peripheral blood mononucleated cells (PBMCs) up to the optimum applied concentration of MgO NPs, and thus may be considered a completely new anticancer agent. MgO NPs-mediated apoptosis was facilitated in cancer cells by the generation of reactive oxygen species (ROS). MgO NPs may show greater plasma distribution in cancer cells and mediate apoptosis via ROS induction [84].

Biodegradable poly(L-lactide) has been widely used in various biomedical applications. However, it has limited applicability due to its poor mechanical properties and acid-induced cell inflammation caused by acidic byproducts during biodegradation [85]. A unique oligo-D-

lactide-grafted magnesium hydroxide (MgO-ODLA) film is synthesized and blended with a PLLA film, and their in-vitro cytotoxicity and inflammation effect is investigated. The probable 2D structure of the MgO-ODLA/PLLA composite is shown in figure 3. The basic MgO-ODLAs composite neutralizes cell cytotoxicity and acid-induced inflammatory response. The MgO-ODLA/PLLA composite has the potential to surpass the drawbacks of PLLA films in the medical field.

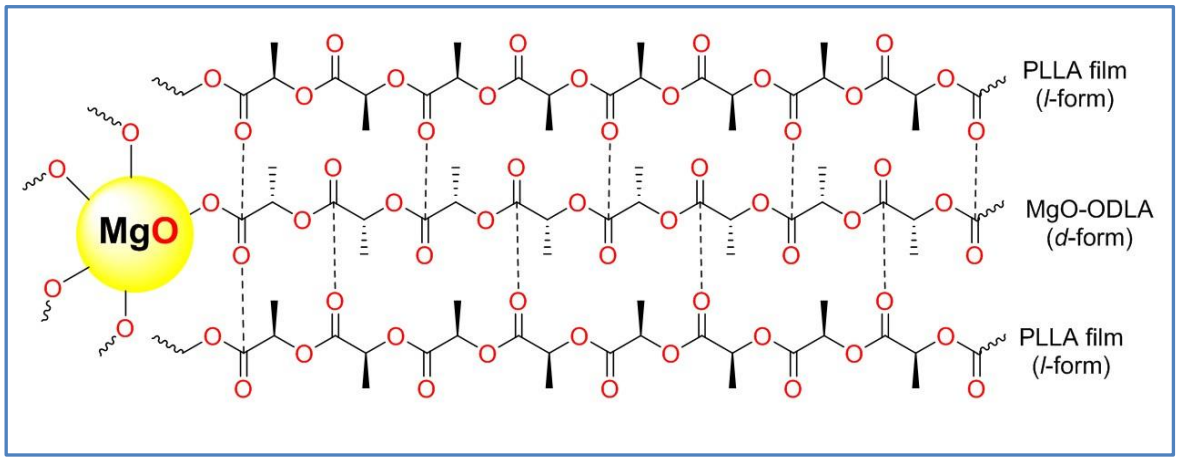

Figure 3. Probable 2D structure of MgO-ODLA/PLLA composite**.**

The drug 5-fluorouracil (5-FC) has been reported to be a potent anticancer agent against various cancers, including breast, stomach, pancreas, colon, and rectum cancer [86]. However, it has some drawbacks for use as a drug, including poor selectivity, impairs normal cells, over-dosage of the drug, and very high diffusion rate, necessitating multiple dosages' intake, and its low solubility characteristics [87]. As a result, it can be delivered by loading it onto a potential drug or delivery system with dose management, vigorously pursued, targeted pathways, and a progressive diffuse rate [88]. Advance carriers, such as nanomaterials, improve drug solubility, control release, promote selectivity at specific sites, reduce degradation rate, improve medicinal profiles, and maintain therapeutic concentrations of drugs in the body [89]. Some carriers for 5-FC have been reported: biopolymers, zeolite, patterned double hydroxides, MCM-based composite materials, kaolinite, halloysite minerals, and clays and their composite materials [90].

Nano-MgO is a non-toxic, secure, low-cost, bioresorbable, and excellent biocompatibility material with potential medicinal applications. Green-synthesized nano-MgO particles were decorated with natural zeolites such as clinoptilolite, yielding a good potential hybrid structure (nano-MgO/Clino) with better absorption capacity, reactivity, biocompatibility, biodegradability, and enhanced 5-FC loading capacity, drug-releasing ability, and automatically cytotoxicity properties. This material has a loading capacity of 244.5 mg/g, greater than clinoptilolite. When compared to free 5-FC, nano-MgO/Clino loaded with 5-FC was found to be secure and have excellent biocompatibility against colorectal normal cells (CCD-18Co) and to have a significant cytotoxic impact on colon cancer cells (HCT-116) [91].

Another research used radiation-induced copolymerization and crosslinking to create a nanoparticle hydrogel from magnesium oxide (MgO) nanomaterials and the natural polymer-based copolymer of Xanthan gum (Xan) and acrylic acid (AAc). It was employed to deliver the drug methotrexate (MTX), used to treat tumors and autoimmune diseases [92]. Direct administration of MTX has some drawbacks, including rapid metabolism and removal from the body, adverse bio-distribution, and low selectivity of medicinal use. MgO nanoparticles

increased network porosity while slightly decreasing gelation and swelling degrees. This addition also regulates the drug-releasing properties of the hydrogel. Including nano-MgO into (Xan-AAc) hydrogel improved drug loading efficiency and lease efficiency, which was highest in the simulated intestine medium (pH 7). The loading efficiency of methotrexate elevated as the nano-MgO content increased. The (Xan-AAc)/MgO carriers enhance Methotrexate delivery while minimizing toxicity, protecting drug bioactivity, extending the duration of action, improving hydrophilicity, and controlling the rate and zone specificity of the released drug.

2-methoxy-estradiol has anticancer activity against various reproductive tract cancers, including the ovary, endometrium, cervix, and prostate. On tumor cells, it has antiangiogenic, anti-proliferative, or apoptotic effects [93]. However, it has an unfavorable kinetic, is poorly soluble in water, is rapidly eliminated, and has poor bioavailability [94]. As a result, it can be administered by using nanoparticles (NPs) as drug delivery carriers, enhancing biological variables without affecting the drug's anticancer properties. To improve the intended selectivity of the anticancer drug 2-Methoxyestradiol (2ME), a novel carrier was created using nano-MgO particles and the polymer polyethylene glycol (PEG) [95].

MgO-PEG-2ME NPs were incorporated with 98.5% 2-Methoxyestradiol and were continuously released over 7 days at pH 2, 5, and 7.35. At 96 hours, the release of 2ME reached a maximum of 2.95 µM, corresponding to 89.27 % of the total 2ME infused into MgO-PEG NPs. These composites reduced the viability of the prostate cancer cell line LNCap and demonstrated anticancer activity comparable to 2ME alone, making them suitable for anticancer prostate therapy. Nano-MgO particles can destroy cancerous cells such as HeLa, AGS, and SNU-16 cells, and the cause of cell death due to MgO exposure has been explained [96]. A schematic representation of MgO-PEG-2ME NPs is shown in figure 4.

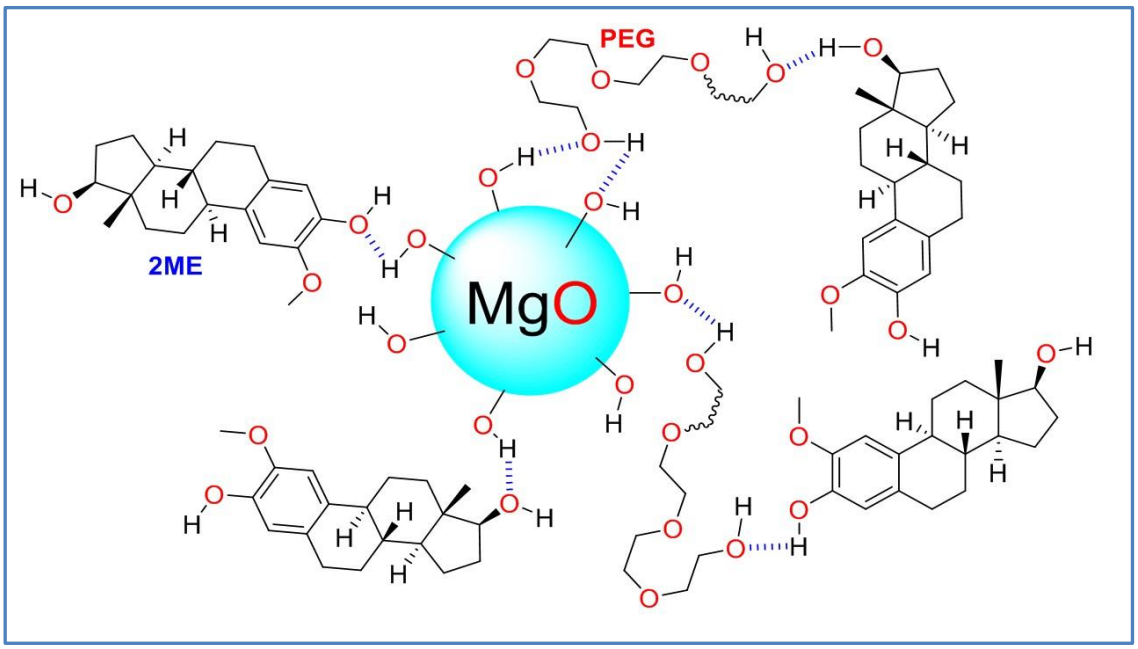

Figure 4. Schematic representation of MgO-PEG-2ME NPs.

According to She *et al*., a decrease in erythropoietin (EPO) hormone levels is linked to kidney function and structure deterioration. This hormone plays a direct and critical role in renal protection by binding and activating the erythropoietin hormone receptor and suppressing apoptosis in kidney cells [97]. The nanoparticles' small size allows them to bind to proteins easily [98]. The nanoparticle-loaded erythropoietin hormone demonstrated high effectiveness

and a relatively long effect period in the human body [99]. Internalization and bioactivity of rhuEPO, when administered into the skin, are limited due to increasingly uncomfortable absorbance into the skin due to the very low permeability; thus, it should be loaded, or rhuEPO-nano-particle conjugate is used, which has good skin permeation properties and gave transdermal protein distribution efficiency [100].

A nano-MgO with an average particle size of 10.8-12.6 nm was prepared chemically and characterized using XRD and TEM techniques, as well as their effect on erythropoietin hormone in blood in-vitro of DKD patients with anemia studied [101]. For the study, blood samples were taken from 24 diabetic patients, 24 diabetic kidney disease patients, and a control group of 20 healthy individuals aged 34 to 72. The study's findings show a significant rise in the amount of erythropoietin hormone in patients with diabetic kidney disease (DKD) who were given MgO NPs versus patients who were not given MgO NPs. There is a nearly 84% noticeable impact on enhancing and activating erythropoietin hormone action. Different physiological correlations predict that when kidney failure occurs, the hormone erythropoietin declines, causing a reduction in hemoglobin and anemia. The rise in erythropoietin activity suggests that nano-MgO affects erythropoietin hormone and its receptor to improve their action, i.e., it may bind and interact with erythropoietin hormone and its receptors, forming their receptor-hormone complex. However, no such connection was discovered between urea, creatinine, and GFR in diabetic kidney disease patients. As a result, nano-MgO would control and regulate general physiological and biochemical effects, increasing hemoglobin levels in the blood and decreasing anemia.

Magnesium and zinc oxides have gotten much attention because of their diverse applications, ranging from electronic sensing devices to catalysts in organic synthesis; they have substantial electronic, physical, mechanical, transport, optical, and chemical properties. As a result, researchers have concentrated their efforts on fabricating ZnO-MgO nanomaterials. Compared to conventional materials, bimetal nanomaterials have distinct physical and chemical properties. They have a high surface area to volume ratio, a dense population of corner or edge surface sites (structural defects), a higher proportion of low coordinated sites [102], and limited size, i.e., in nanometer scale, smaller crystallite size, reactivity, and absorption efficiency is higher [103]. Doxorubicin is an essential anticancer drug widely used to treat a variety of cancer cells, including breast carcinoma, lymphomas, acute leukemia, soft tissue, osteogenic sarcomas, and bronchogenic (lung) carcinoma. However, doxorubicin has serious complications such as immune system damage, hearing failures, serious vomiting, intense nausea, loss of hair, and dermal problems [104].

As a result, many investigators are working to develop drug carriers that will deliver the drug to the targeted tumor site with minimal side effects. Several other nanoparticles and nanostructured materials were assessed for doxorubicin carriers in the creation of drug delivery systems [105]. Numerous findings have been made on the kinetic study of doxorubicin adsorption on nano-MgO particles and their discharge at various pH levels using various statistical models. A systematic representation of absorption interactions between doxorubicin and MgO nanoparticles is shown in figure 5. It has been reported that as pH decreases, doxorubicin-releasing efficiency increases due to the neutralization of the nano-MgO surface and subsequent dissolution. The Hixson-Crowell model can predict doxo release and nano-MgO dissolution [106].

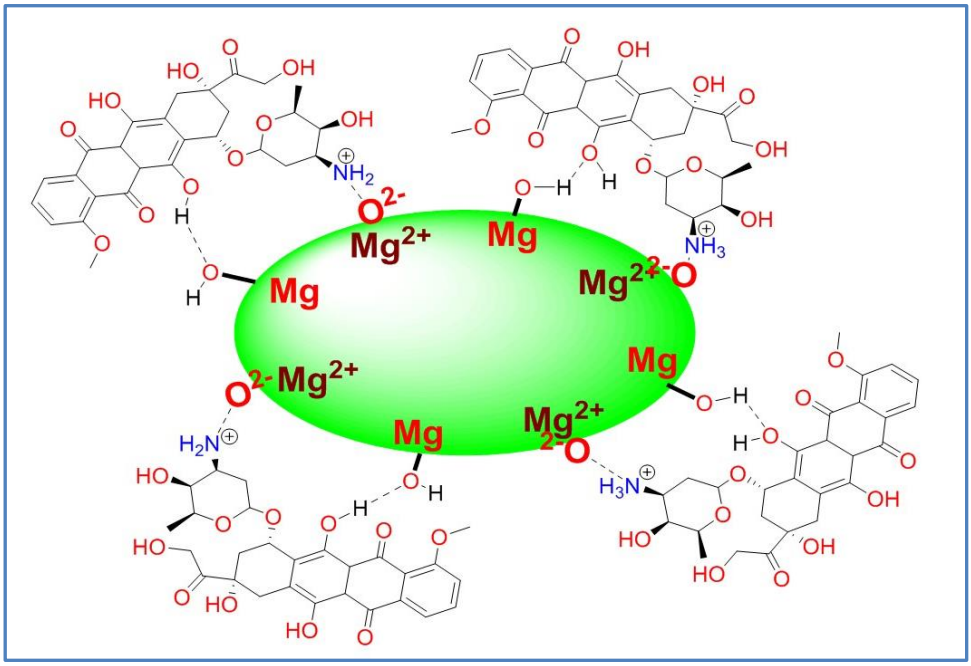

Figure 5. Systematic representation of absorption interactions between doxorubicin and MgO nanoparticles.

Cancer patients are always deficient in minerals, and the drug used to treat them, doxorubicin, has some side effects. An innovative targeted medication delivery system has been created by loading doxorubicin on porous magnesium oxide nanoflakes (drug carriers) [107]. The drug's activity is pH dependent due to the cancer cells' variable extracellular (pH 6.2-6.9, slightly acidic) and intracellular medium pH (7.12-7.65) [108].

The drug loading capacity of magnesium oxide (MgO) nanoflakes is remarkable at 90%, and the drug release rate at the desired target is pH-dependent: 10% at pH 7.2, 50.5% at pH 5.0, and 90.2% at pH 3. The major benefit of this TDD system is that it does not disintegrate at the physiological pH of blood (7.2), and drug release is very low during the transfer process, reducing the drug's cytotoxicity to healthy cells. The extracellular medium of cancerous cells has a slightly acidic pH, the drug discharging effectiveness is average, and MgO nanoflakes degrade (i.e., dissolve) gradually and release magnesium ions to the cancerous region. This TDD system is used to overcome hypomagnesemia while minimizing cytotoxicity to healthy cells.

In a dark room at room temperature, a new bimetal MgO-ZnO nanocomposite has been synthesized by precipitation method, and its effectiveness in absorbing and releasing anticancer drugs such as doxorubicin was studied [109]. Due to the obvious strong affinity between doxorubicin and nanomaterials, hydrogen bonding, and electrostatic interaction among positively charged doxorubicin molecules and negatively charged surface of ZnO-MgO nanoparticles, the drug molecules are subsumed over the surface of the nanomaterial. At neutral pH, 14% of doxorubicin is released from the surface of nanoparticles, whereas at acidic pH 4, nearly 68% of doxorubicin is released at 6.5 hours due to dissolution and neutralization of the surface charge of ZnO-MgO nanoparticles. This finding suggests the drug is released quicker at acidic pH 4 than at neutral pH. According to the study, ZnO-MgO nanoparticles will be used as a promising carrier in drug delivery systems after further biological and pharmacological research. A systematic representation of absorption interactions between doxorubicin and ZnO-MgO nanoparticles is shown in figure 6.

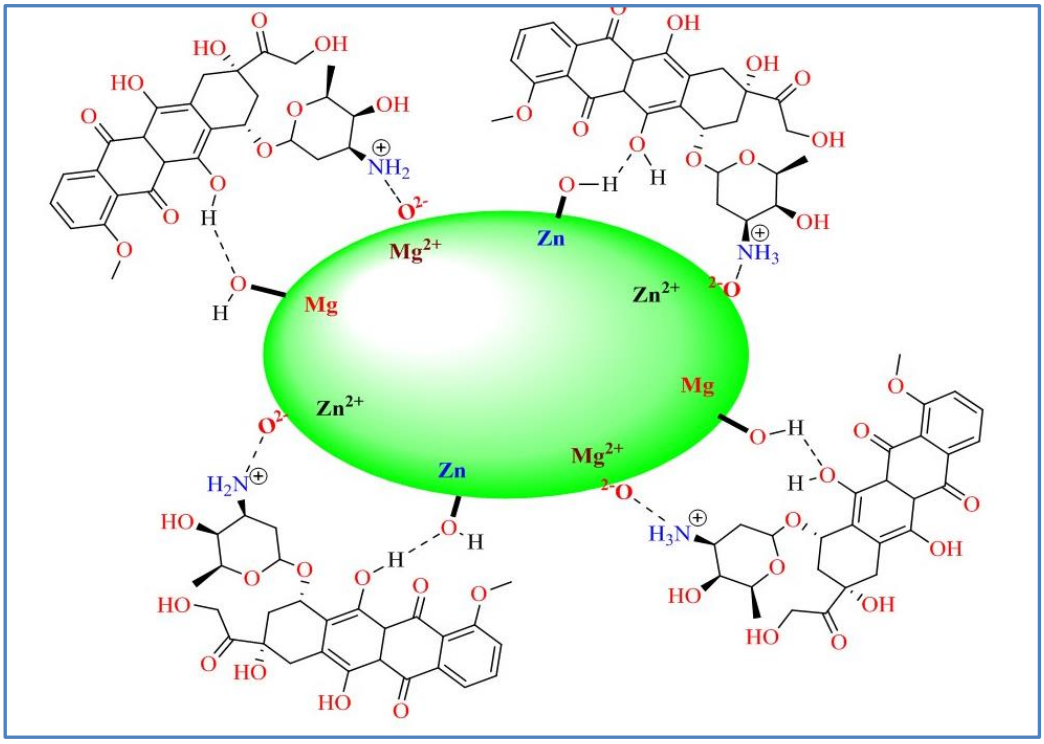

Figure 6. Systematic representation of absorption interactions between doxorubicin and ZnO-MgO nanoparticles.

Using $Mg(NO_3)_2.6H_2O$ and silver nitrate, pure and Ag (1%, 2%, 5%, 7.5 % mol)-doped MgO NPs were prepared using a simple sol-gel method. The luminescence study confirms that Ag-ions deposit on the surface of nano-Mgo; the intensity of the excitation and emission of light significantly reduces as the Ag content increases. The photocatalyst 2% Ag-doped/nano-MgO was discovered to be an outstanding photocatalyst for the UV-degradation of methylene blue dye, decomposing around 75% dye in 180 minutes. Figure 7 depicts the mechanism of photocatalytic degradation of MB dye by Ag-doped MgO NPs. The MTT (cytotoxicity) assay revealed that both pure and Ag-doped MgO NPs were low in toxicity to human normal umbilical vein endothelial cells (HUVECs) [110].

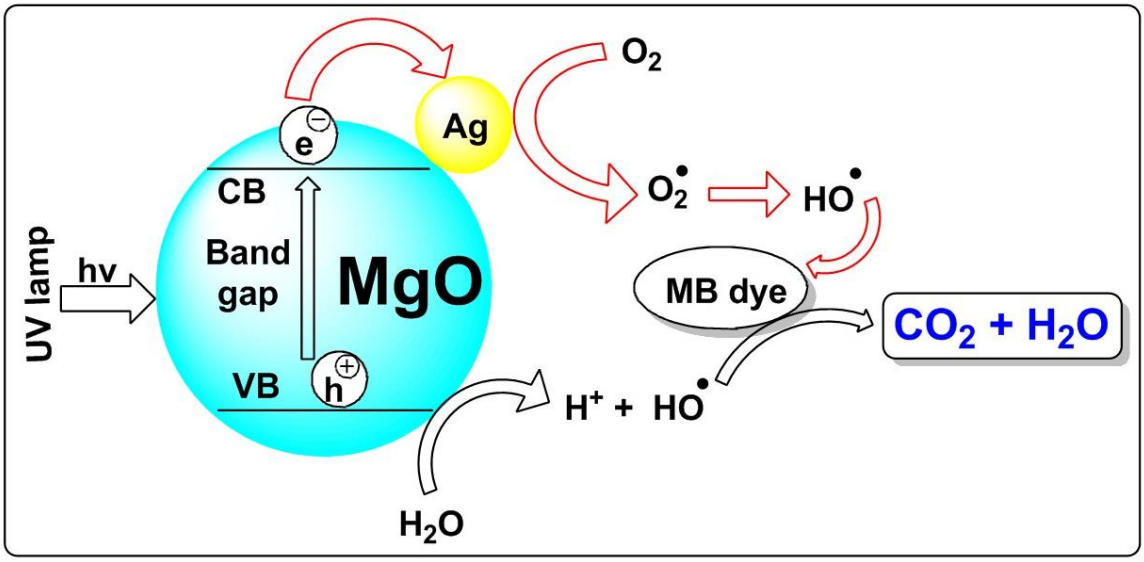

hv ≥ E_g (band gap), conduction band (CB), valance band (VB)

Figure 7. Mechanism of photocatalytic degradation of MB dye by Ag-doped MgO NPs [110].

CsI(Na)@MgO-and-5-ALA combination was reported for Radio-dynamic therapy (RDT) [111]. The CsI(Na)@MgO and 5-ALA conjugates evaluated in vitro against 4T1 cells increased radiation-induced ROS, which increases DNA, mitochondrial, and lipid damage, ultimately reducing cell proliferation and clonogenicity. This treatment reduced tumor cell numbers quantitatively. The low-toxic ingredients, low toxic alkali and halide elements were effectively removed from the body after treatment, and no harmful side effects were observed in the host.

An aqueous solution of nano-MgO with low toxicity exhibits encouraging antimicrobial activity both *ex-vivo* and *in-vitro*. Compared to sodium hypochlorite, 5 mg per liter aqueous solution of nano-MgO exhibited remarkable long-term efficiency for *E. faecalis* inhibition. To shed light on other aspects of antibacterial activity, it must be able to remove the smear layer, penetrate the dentinal tubes, and dissolve pulpal and necrotic tissues. It has been used as a root canal irritant and has no cytotoxicity [112].

Several other reports on nano-MgO fabrication from plant extracts containing active biomedical phytochemicals with promising biomedical applications. Green nano-MgO rod particles (average diameter around 50 nm) were synthesized in an aqueous medium using *Gmelina arborea* fruit extract (GAE) and tested for anticancer efficacy against the MCF-7 breast cancer cell line. At 400 g/mL concentration, these nanoparticles inhibit cells by up to 96% [113].

2.4. Alzheimer's disease.

Alzheimer's disease is an age-related progressive neurodegenerative condition that is primarily observed in Alzheimer's disease patients due to continuous exposure to toxic metals such as aluminum present in the environment. This affects the brain depending on the route of intake, level of exposure [114], and time and usually causes dysfunction of the central cholinergic system (enzyme, AChE), which plays an important role in memory, cognitive, and learning functions [115]. Ach is affected by the enzyme AChE. With Al exposure or in Al-intoxicated albino rats, ACh and AChE levels decrease. The interaction of Al with the peripheral sites and secondary structure of AChE reduces its activity.

Curcumin was employed to treat and prevent Alzheimer's disease because it penetrates the central nervous system [116], attenuates neuropathological changes in the hippocampus, and inhibits apoptosis [117]. However, curcumin's low aqueous solubility, poor gastrointestinal absorption, rapid metabolism, and alkaline pH degradation reduce curcumin's bioavailability, limiting its utilization in treatments. Nanotechnology was used for nano-based target delivery of curcumin using a nano-carrier at infection sites, which increased bioavailability in the organism, improved diagnostic accuracy, and reduced toxicity [118].

Inorganic CuMgO nano-particles, for instance, were used for drug delivery due to their biodegradability, biocompatibility, and low price, with greater encapsulation of active drugs and minimal drug loss during circulation. Previous research has shown that the beneficial or negative effects of nano-MgO particles depend on particle concentration, particle composition, particle size, surface area [119], duration of exposure time [120], nature of the biological target, and particle compactness [121].

CuMgONPs at 500 µg/ml demonstrated effective delivery, significantly increasing Ach and AChE levels. The effects of Al + CuMgONPs diagnosis on AChE levels in the cerebral cortex (19.54%), cerebellum (16.65%), and ACh levels in the cerebellum (25.54%) were significant ($P < 0.000$) when compared to the Al alone, treated group. CuMgONPs balancing

cholinergic levels demonstrated a strong correlation with an increase in total antioxidant levels. The toxic effects of increased MgONps concentrations above 200 µg/ml are reversed by loading NPs with curcumin (potent antioxidant and neuroprotective agent). MgONPs act as a curcumin carrier and have been shown to have antioxidant properties, anticancer properties, and antidiabetic impacts in rat pancreatic islets [122], as well as Mg in metallic form having neuroprotective effects and lowering LPO after spinal cord injuries in rats [123]. CuMgONPs + Al significantly enhanced the total histoarchitecture of the cerebral cortex and the cerebellum. Furthermore, Al + CuMgONPs administered with Curcumin completely reversed Al's effect [124].

2.5. Mg^{2+} ions delivery/bone repairing mechanism.

Patients with broken bones, especially those with osteoporosis, needed a prolonged period for bone formation [125]. As a result, efforts have been made to shorten the period of bone healing by using growth factors such as recombinant human bone morphogenetic proteins 2 (rh-BMP2) as drugs [126]. However, using a large dose or concentration causes cell apoptosis in human primary periosteal cells and is detrimental to cell proliferation [127]. Long-term use of some other anti-catabolic bisphosphonate drug causes fragile, hypermineralized bones that are effortlessly fractured [128]. Mg^{2+} ions play a significant role in creating biological apatite and in the connection and differentiation of osteoblastic cells [129].

They are also involved in mineralization, which controls bone formation and resorption [130]. However, high doses or concentrations of Mg^{2+} ions (>5.0mM) hurt human osseous metabolism, osteoblast differentiation, and homeostasis, leading to osteomalacic renal osteodystrophy, bone mineralization deformities, and associated bone diseases [131]. As a result, complete control of extracellular Mg concentration is compelled for bone formation. As a result, an approach for controlling the release of Mg^{2+} ions to stimulate bone formation has been reported. For 22 days, a dip coating (Mg/Epoxy resin-ZnO/PCL-Ibuprofen) on magnesium alloy released both Mg^{2+} and ibuprofen in PBS [132].

A novel highly dispersed PLGA/MgO-alginate core-shell microsphere system was created using a uniquely engineered microfluidic capillary device and poly (lactic-co-glycolic acid) (PLGA), alginate, and nano-MgO particles. It can boost osteoblastic activity in vitro and encourage new bone formation by releasing magnesium ions in situ [133]. In rat models, a PLGA/MgO-alginate core-shell microsphere system exhibits great cytocompatibility and, *in situ*, new bone formation.

Controlled drug discharge at the site of the infection is accomplished through the use of biodegradable, FDA-approved, and biocompatible polymeric poly (lactic-co-glycolic acid) (PLGA) nanoparticle, PLGA/chitosan microparticles, and PLGA/chitosan/MgO microparticles. Surface treatment of PLGA with other hydrophilic polymers is used to create controlled-release drug delivery composites. However, the hydrophilic surface of PLGA hurts therapeutic outcomes. As a result, PLGA/chitosan microparticles were created to control the release of medications. The modified double emulsion solvent evaporation method created PLGA/chitosan microparticles. It was additionally refined with magnesium oxide and used to treat Mg deficiency. MgO encapsulated in PLGA and PLGA/chitosan microparticles were employed for the controlled release of Mg^{2+} and the treatment of Mg insufficiency [134].

MgO was hydrolyzed radially to magnesium hydroxide with no hydrogen loss [135]—the inclusion of 3 wt.% MgO nanoparticles to PLA to create a nano-MgO/PLA composite enhanced the pH of the deterioration media and, more pertinently, enhanced the proliferation

profile of MC3T3-E1 murine osteoblasts, potentially by increasing the basicity at the composite surface, which promotes osteoblast growth [136]. Nanofibers made of nano-MgO/polycaprolactone (PCL) composite were created. The PCL fiber diameters decrease significantly as the concentration of MgO particles increases. Including nano-MgO tends to increase the hydrophilic nature of PCL while also increasing their bioactivity. When contrasted to ADSCs on pure PCL electrospun scaffolds, nano-MgO/PCL electrospun scaffolds increased osteogenic differentiation by significantly increasing Ca-deposition, ALP activity ($P < 0.05$), and osteogenic-related gene expressions (Col1a1 and OPN) ($P < 0.05$). As a result, nano-MgO/PCL hybrid composites could be good fits for ADSC osteogenic differentiation and bone tissue engineering [137]. Another biodegradable nanofiber made of biodegradable phosphate glass fiber, polylactic acid (PGF/PLA), and nano-MgO can be used as bone tissue engineering scaffolds since it discharges Ca, P, and Mg during degradation, promoting bone repair. The nano-MgO was a neutralizing agent to keep the pH close to physiological levels. MgO neutralized the acidic biodegradable product, hindering the strenuous deterioration of PGF in the acidic medium. For bone tissue engineering, the (MgO + PGF)/PLA composite was chosen [138].

A novel fabrication of poly (lactic acid) (PLA) electrospun fibers loaded with 10 and 20 wt% bioactive glass (n-BG) and magnesium oxide (nano-MgO) nanoparticles of size 27 and 23 nm, respectively, and their application in bone tissue engineering are being investigated. Both of these nanomaterials work synergistically to improve bactericidal behavior and bioactivity. Because of the precipitation creation of hydroxyapatite structure on the surface, PLA-n-BG composites demonstrated bioactivity. PLA/n-BG and PLA/nano-MgO demonstrated little or no antimicrobial activity. The distinct composites boost the production of alkaline phosphatase (ALP) in contrast to pure PLA, affecting cell viability, i.e., an excellent osteoblastic phenotype expression capacity with the PLA-n-BG showing the highest osteoblastic expression [139].

The number of people diagnosed with bone defects is growing due to a variety of factors such as population aging, infections, biological disorders, vehicle accidents, and so on. To improve PLA's shortcomings and clinical applications, two kinds of surface-modified whiskers, grafted-MgO and chitin (CHN), were grafted onto a poly(L-lactide) (PLLA) matrix individually or together to produce PLLA/g-MgO/g-CHN composite films and bone nails via injection molding [140]. Cross-linking by H-bonding and electrostatic interactions scattered the grafted whiskers homogeneously on the PLLA matrix. Grafting with g-MgO and g-CHN wrinkles enhanced the hydrophilicity, cell adhesion, proliferation, cell cycle alteration, the decline in cell apoptotic rate, and cytocompatibility of the PLLA matrix [141]. When compared to the pure PLLA, PLLA/g-MgO, and PLLA/g-CHN films, the PLLA/g-MgO/g-CHN film improved expanding and cell adhesion, the proliferation of mouse embryo osteoblast precursor (MC3T3-E1) cells, cell-cycle alteration, and inhibition of cell apoptosis. The PLLA/g-MgO/g-CHN group had a higher level of calcium deposition, calcification of cells, and ALP secretion in vitro, as well as expression of osteogenesis genes (ALP, Runx-2, COL I, OCN) than the other PLLA composite and PLLA groups. The increased osteogenesis may aid in other-related genes' mRNA and protein expression. This supports the synergistic stimulating effect of g-MgO and g-CHN whiskers on osteogenic differentiation and PLLA matrix cell affinity. After 16 weeks of implant placement, new bone formation was spotted in rabbits implanted with PLLA, and PLLA composite bone nails are higher in the PLLA/g-MgO/g-CHN group. Furthermore, the bending strength of broken bone repaired by PLLA/g-MgO/g-CHN bone nail

is 48 MPa, greater than that of other bone nail groups. These results imply that combining g-MgO and g-CHN whiskers in a PLLA matrix plays a favorable role in cell affinity and osteogenic differentiation and that the formed PLLA/g-MgO/g-CHN composites have immense promise in bone repair fields [142].

Another research used *in situ* polymerization to create poly(l-lactide)-magnesium oxide whiskers composites and examined their bone repair efficiency and implantability [143]. The nano-MgO was evenly distributed in the PLLA matrix using various secondary forces. The study demonstrates that nano-MgO influences the in-vivo deterioration of PLLA-nano-MgO composites. A whisker content of 0.5 wt% and 1.0 wt% demonstrated a significant nucleation effect for the PLLA matrix, and 1.0 wt% of nano-MgO demonstrates an excellent improvement in the mechanical properties of the composites. Dispersed nano-MgO regularities the deterioration of the PLLA matrix while increasing its bioactivity, implying that the PLLA-MgO composite could be used as a biomedical substance for bone-related repair. Nano-MgO particles enhance the mechanical characteristics of PLLA composite scaffolds while improving bone-cell proliferation and adhesion [144].

Nano-MgO and chitin whiskers transplanted to PLLA and pure PLLA were tested for in vitro dissolution behavior in PBS solution with a pH of 7.4 at 37.5°C. The g-MgO accelerates the way earlier degradation of the composite, whereas the g-CHNs/PLLA composite accelerates the later degradation. Both materials are added to sustain the mechanical strains of the composite early on, but they stimulate later on. The g-MgOs/g-CHNs/PLLA composite's tunable degradation behavior is critical for its use as a bone internal fixation implant [145]. Some other functionalized degradable copolymer, poly(L-lactide-co-malic acid) (PLMA), is synthesized. It has better cell adhesion and affinity [146] and degrades faster than neat PLLA [147]. The free hydroxyl groups on the surface of nano-MgO particles formed carboxylates easily with the hydrophilic carboxyl group of PLMA. To acquire modified m-MgO-NPs, PLMA with a pendent carboxyl group (primarily from malic acid) is grafted (nearly 27%) over the surface of nano-MgO particles via carboxylate linkage. The resulting m-MgO-NPs were employed as a nucleating agent or padding and integrated into the PLLA matrix to improve mechanical properties, reduce the contacting angle and degradation rate of the PLLA, and increase cell viability. As a result, the PLLA/m-MgO-NPs biocomposite material has great promise for bone repair and implant material fixation [148].

MgO nanomaterials in the 40-60 nm size range are synthesized using the traditional precipitation-calcination method and loaded onto the polycaprolactone (PCL) polymer to produce MgO-enriched PCL composite scaffolds. This nano-filler is uniformly dispersed on the polymer fiber, which improves the mechanical properties of nanomaterials (tensile strength and elastic modulus). When compared to neat PCL scaffolds, the nano-MgO-PCL electrospun composite exhibits impressive in-vitro bioactivity in terms of deterioration, mineralization, bioactive Mg ion discharge, biocompatibility, rougher surface morphology, nanoscale topography, and enhanced hydrophilicity. By the third day of incubation, it had formed a surface hydroxyapatite layer. An in-vivo subcutaneous implantation study in SD rats reveals a medium inflammatory tissue response at the implantation surface in the second week without any toxic effects on vital organs, as well as no substantial change of blood and serum biochemistry variables from the normal clinical range. According to the research findings, nano-MgO-PCL composite electrospun fibers could be seen as an effective scaffold material for bone-soft tissue engineering applications, including ceramic filler and preparing different biomedical scaffold applications [149]. Given the favorable advancement in tensile strength of

basic polycaprolactone-keratin blends, nano-MgO particles composite with polycaprolactone-keratin blends have been employed in tissue engineering applications, according to another study [150].

Electrospinning was used to create polycaprolactone (PCL)/magnesium oxide (MgO)/graphene oxide (GO) nanofibers composite materials, which were then tested for biocompatibility and osteogenic distinction of adipose-derived mesenchymal stem cells (MSCs) [151]. Adding GO with oxygen-containing functional groups and nano-MgO particles alters nanocomposites' surface roughness and hydrophilicity, promoting cell adhesion, proliferation, and differentiation. MSC adherence, spreading/viability, and ALP activity (proliferation) are improved by PCL/MgO/GO composites over pure PCL. Furthermore, the utterance of osteogenic markers such as runx2, Col1a1, and OPN increased (by more than 2-fold) in cells sown with PCL/MgO/GO composites. The GO and nano-MgO particles enhanced the biocompatibility of the PCL scaffold and increased MSC osteogenic differentiation.

Because of its biocompatibility and high overall strength, hydroxyapatite ($Ca_{10}(PO_4)_6(OH)_2$, HAp, ceramic material) has been employed for osteoconductive bone implants. A polycaprolactone (PCL)/HAp composite was created by adding nano-MgO and then etching it with oxygen and nitrogen plasma under anisotropic circumstances [152]. Introducing 1-15% MgO/HAp nanomaterials to PCL and plasma treatment impacted preosteoblast cell behaviors such as proliferation, adhesion, and differentiation of MC3T3-E1 cells. Nitrogen plasma-treated 3D PCL/HAp/nano-MgO composites demonstrated the greatest bioactivity among all samples.

The mechanical properties, deterioration properties, hydrophilicity, and osteogenic activity of a new PLA matrix with nHA/nano-MgO porous composites were assessed using digital model design and 3D printing techniques. Nano-MgO improves permeability, crystallinity, and mechanical properties. The increase in pH was beneficial to osteoblast growth, and osteoblasts could mineralize efficaciously at pH = 8.0 [153]. The material decomposes slowly, and the nanomaterials are hydrolyzed to a small extent. It has been suggested for bone tissue engineering repair [154]. Through blending extrusion, a novel polylactic acid (PLA)/stearic acid-modified 1% magnesium oxide (MgO) composite was created, and the impact of nano-MgO shape on composition in vitro and in vivo degradation was explored [155]. The form of the filler had an impact on the long-term deterioration of the composite, including nano-MgO, which increases the hydrophilicity of composite materials and expedites degradation. In addition, the pH of the phosphate buffer solution (PBS) was retained or controlled by dissolving MgO, which neutralized the acidic product produced by long-term PLA degradation. As a result, a (PLA)/stearic acid-modified 1% magnesium oxide (MgO) composite could be used for bone repair.

2.6. Antidiabetic activity.

Nano-MgO particles improved and activated erythropoietin hormone action by approximately 84.8% in patients with DKD-associated anemia. Several findings illustrate the importance of nano-MgO in reducing serum glucose and lipid manufacturing in diabetes treatment. Aptamers are single-stranded oligonucleotides composed of either DNA or RNA with a strong affinity for cognate target molecules, resulting in 3D conformational structures [156]. It has special features such as thermal and chemical stability, greater specificity and sensitivity bioavailability, and an enticing affinity for ligands; all combine to make it an effective drug delivery and in-vivo cell targeting agent [157]. However, some biochemical and

biophysical barriers persist for the real-world applications of aptamer-mediated cell targeting strategies, including serum degradation due to the tiny size of the aptamers, the aptamer-cell membrane barrier, and rapid systemic clearance [158]. These challenges were partially overcome by employing biodegradable polymeric vessels that lead to the transfer and defense of ligand and drug molecules during cellular trafficking. Anti-PDGF aptamer conjugated-E10030 drug encapsulated PEG formulation (neovascular age-related muscular degeneration), nucleolin-targeting AS1411 polymeric system are two examples (myeloid leukemia, glioma, and breast cancer) [159], EpCAM-conjugated PEI nanoparticles (breast and retinoblastoma tumors) [160], A10 RNA aptamer-linked PLGA-PEG particles (targeting prostate cancer cells) [161]. For the delivery of embedded nanoparticles containing magnesium oxide to diabetic 3T3L1 cell lines, an aptamer-navigated polymeric system (DPAP) was also employed [162]. Even though DPAP is less toxic than the most commonly used polymers, PLGA and PEI, it was chosen to prepare anti-diabetic nanomaterials [163].

Multifunctional DPAP is created by copolymerizing PLGA and PEI and incorporating a thrombin-specific DNA aptamer. It is a particulate delivery layer-by-layer organized system with the drug, i.e., nano-MgO particles synthesized by chemical and green methodologies (payload D), encased within the inner polymeric core of PLGA, i.e., particulate delivery layer by layer organized system (P). As the specific target elements, thrombin-specific DNA aptamer molecules are covalently linked onto the surface of the PLGA layer, i.e., (A). Finally, the PEI polymeric molecules are infiltrated with the aptamer as the outermost layer (P). These samples were 3T3-L1 diabetic cells that were researched for in vitro performance measures such as aiming capability, drug entrapment, insulin reversal ability, and cellular transcriptional activator. The green synthesis of DPAP-nano-Mg_2O has a higher encapsulation efficiency and loading ability of 93.69% and 0.03 mg MgO/mg PLGA, respectively. Both samples improved in vitro cellular uptake as well as the ability of 3T3-L1 cells to reverse insulin resistance. Figure 8 depicts the synthesis and proposed mechanism of DPAP-nano-MgO targeted drug delivery & development of insulin resistance reversal in 3T3-L1 adipose cell lines.

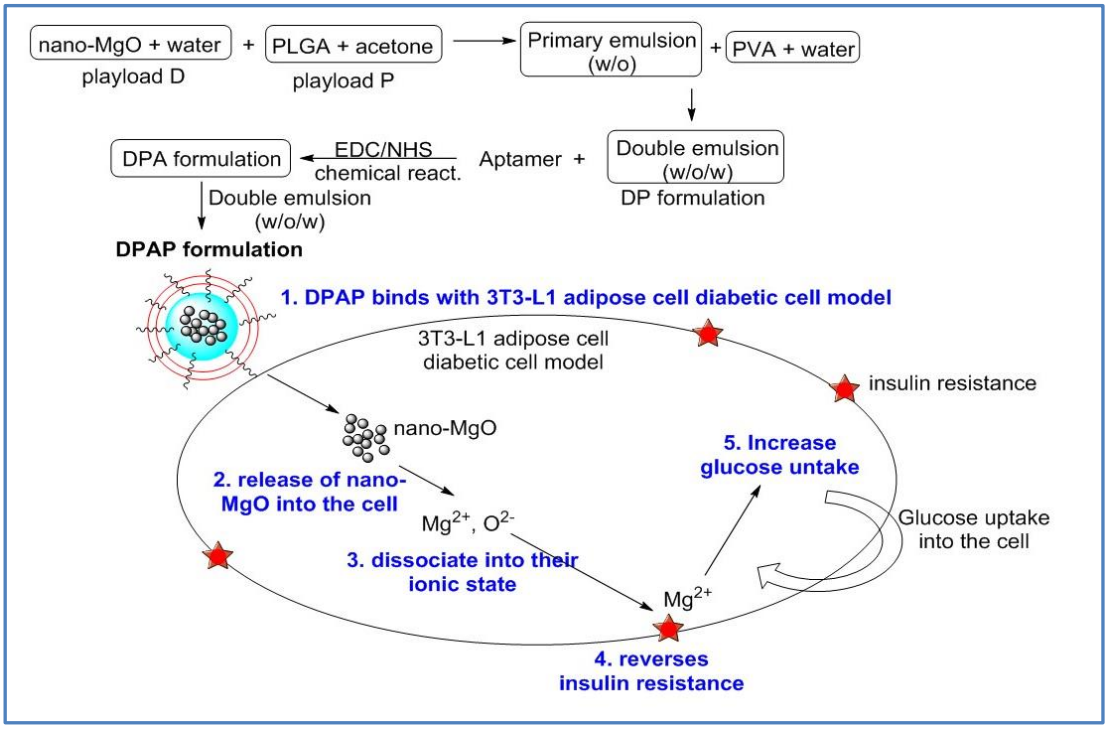

Figure 8. Synthesis and proposed mechanism of DPAP-nano-MgO targeted drug delivery & development of insulin resistance reversal in 3T3-L1 adipose cell lines.

3. Conclusion

Magnesium oxide (MgO) nanoparticles have been synthesized by chemical and biochemical methods using magnesium chloride, magnesium acetate, and magnesium nitrate as catalysts. Nano MgO possesses optimum surface area and active reaction sites. MgO nanocomposites have prominent medical applications, including antibacterial, anti-cancer, anti-inflammatory, bone-repairing mechanisms, anti-diabetics, cytotoxicity, and drug delivery. Because of their high strength-to-weight ratio and good biocompatibility in all mediums, nano-MgO composites are used in bone implants, biodegradable fibers, and screws. Nano MgO has optimum biocompatibility due to its less toxic nature. It is also used with other nanocomposites, and its physicochemical properties change with the doping of other metals or metal oxides. As a result, the surface area or structural defects of nano-MgO are significant features to consider when designing MgO-containing medical devices.

Funding

No funding was received.

Acknowledgments

The contributors to this work, whether directly or indirectly, have our sincere gratitude.

Conflicts of Interest

The authors declare no conflict of interest.

References

1. Salem S.S.; Hammad; E.N.; Mohamed, A.A.; El-Dougdoug, W. A Comprehensive Review of Nanomaterials: Types, Synthesis, Characterization, and Applications. *Biointerface Res. Appl. Chem.* **2023**, *13*, 41, https://doi.org/10.33263/BRIAC131.041
2. Gupta, D.; Boora, A.; Thakur,A.; Gupta, T.K. Green and sustainable synthesis of nanomaterials: Recent advancements and limitations. *Environ. Res.* **2023**, *231*, 116316, https://doi.org/10.1016/j.envres.2023.116316.
3. Abdussalam-Mohammed, W.; Abraheem, M.S.; Mezoughi, A.B.; Mohamed, L.; Alwahsh, M.A.A. Comparative Analysis of Novel Iron Oxide Nanoparticles Synthesized by Different Approaches with Evaluation of Their Antibacterial Activities. *Biointerface Res. Appl. Chem.* **2023**, *13*, 317, https://doi.org/10.33263/BRIAC134.317 .
4. Husain, Q. An overview on the green synthesis of nanoparticles and other nano-materials using enzymes and their potential applications. *Biointerface Res. Appl. Chem.* **2019**, *9*, 4255-4271, https://doi.org/10.33263/BRIAC95.255271 .
5. Tripathy, P.; Sethi, S.; Panchal, D.; Prakash, O.; Sharma, A.; Mondal, R.B.; Pal, S. Chapter 13 - Biogenic synthesis of nanoparticles by amalgamating microbial endophytes: potential environmental applications and future perspectives. In Microbial Endophytes and Plant Growth, Solanki, M.K.; Yadav, M.K.; Pratap Singh, B.; Kumar Gupta, V., Eds., Academic Press, **2023**; 215-231, https://doi.org/10.1016/B978-0-323-90620-3.00003-9.
6. Waiezi, S.; Nizam, N.A.N.M.; Asraf, M.H.; Sani, N.S. Preparation, Characterization, and Antibacterial Activity of Green-Biosynthesised Silver Nanoparticles using *Clinacanthus nutans* Extract. *Biointerface Res. Appl. Chem.* **2023**, *13*, 171, https://doi.org/10.33263/BRIAC132.171.
7. Mohammed, K.J.; Hadrawi, S.K.; Kianfar, E. Synthesis and Modification of Nanoparticles with Ionic Liquids: a Review. *BioNanoSci* **2023**, *13*, 760–783, https://doi.org/10.1007/s12668-023-01075-4.

8. Sheela, L.S.; Jebasingh, B; Manickam, V; Sumathi, J.; Benedict, B.A. Electrochemical Synthesis and Characterization of MgO Nano Particles: A Comparative Catalytic Activity of Different Methods of Synthesis. **2023**; http://dx.doi.org/10.2139/ssrn.4442567.
9. Wei, L.; Gao, Z. Recent research advances on corrosion mechanism and protection, and novel coating materials of magnesium alloys: a review. *RSC Adv.* **2023**, *13*, 8427-8463, https://doi.org/10.1039/d2ra07829e.
10. Kumar, K.; Das, A.; Prasad, S.B. Effect of multi-pass friction stir processing on mechanical, microstructural, bioactivity, and corrosion properties of novel magnesium-hopeite composite for biomedical applications. *Mater. Today Commun.* **2023**, *35*, 105584, https://doi.org/10.1016/j.mtcomm.2023.105584.
11. Yin, S.; Zhou, Z.; Lin, T.; Wang, X. Magnesium Depletion Score is Associated with Long-Term Mortality in Chronic Kidney Diseases: A Prospective Population-Based Cohort Study. *J. Nephrol.* **2023**, *36*, 755–765, https://doi.org/10.1007/s40620-022-01489-5.
12. Gosalia, H.; Patel, O.; Doctor, N.M.; Shah, H. A STUDY OF HYPOMAGNESEMIA IN PATIENTS ADMITTED IN MEDICAL ICU AND ITS CORRELATION WITH FINAL OUTCOME. *Natl. J. Med. Res.* **2023**, *13*, 17–21.
13. Klabunde, K.J.; Stark, J.; Koper, O.; Mohs, C.; Park, D.G.; Decker, S.; Jiang, Y.; Lagadic, I.; Zhang, D. Nanocrystals as Stoichiometric Reagents with Unique Surface Chemistry. *J.Phy. Chem.* **1996**, *100*, 12142–12153, https://doi.org/10.1021/jp960224x.
14. Mazaheri, N.; Naghsh, N.; Karimi, A.; Salavati, H. In vivo Toxicity Investigation of Magnesium Oxide Nanoparticles in Rat for Environmental and Biomedical Applications. *Iran. J. Biotech*. **2019**, *17*, 1-9, https://doi.org/10.21859/ijb.1543.
15. Cohen, M.L. Changing patterns of infectious disease. *Nature* **2000**, *406*, 762-767, https://doi.org/10.1038/35021206.
16. Muteeb, G. Nanotechnology-A Light of Hope for Combating Antibiotic Resistance. *Microorganisms* **2023**, *11*, 1489, https://doi.org/10.3390/microorganisms11061489.
17. Sadoq, B.E.; Britel, M.R.; Bouajaj, A.; Maâlej, R.; Touhami, A.; Abid, M.; Douiri, H.; Touhami, F.; Maurady, A. A Review on Antibacterial Activity of Nanoparticles. *Biointerface Res. Appl. Chem.* **2023**, *13*, 405.
18. Verma, R.K.; Nagar, V.; Sharma, A.; Mavry, B.; Kumari, P.; Lohar, S.; Singhal, A.; Prajapati, M.K.; Singh, A.; Awasthi, K.K; Sankhla, M.S. Green Synthesized Nanoparticles Targeting Antimicrobial Activities. *Biointerface Res. Appl. Chem.* **2023**, *13*, 469, https://doi.org/1.33263/BRIAC135.469.
19. Narayanaswamy, S.; Bhaskar, R.; Jayadevappa, R.K.K.; Ramachandran, S.K.M.; Madhu, A.P. A Comprehensive Review on the Antimicrobial and Photocatalytic Properties of Green Synthesized Silver Nanoparticles. *Lett. Appl. NanoBioScience* **2023**, 12, 140, https://doi.org/10.33263/LIANBS124.140.
20. Patil, T.; Gambhir, R.; Vibhute, A., Tiwari, A.P. Gold Nanoparticles: Synthesis Methods, Functionalization and Biological Applications. *J. Clust. Sci*. **2023**, *34*, 705–725, https://doi.org/10.1007/s10876-022-02287-6.
21. Hameed, H.G.; Abdulrahman, N.A. Synthesis of TiO_2 Nanoparticles by Hydrothermal Method and Characterization of their Antibacterial Activity: Investigation of the Impact of Magnetism on the Photocatalytic Properties of the Nanoparticles. *Phys. Chem. Res.* **2023**, *11*, 771-782.
22. (~~a~~) Giridasappa, A.; Shareef, M.I.; Gopinath, S.M.; Rangappa, D.; Shivaramu, P.D.; Sabbanahalli, C. Synthesis, Antioxidant, Bactericidal and Antihemolytic Activity of Al_2O_3 and SnO_2 Nanoparticles. *Proc. Natl. Acad. Sci., India, Sect. B Biol. Sci.* **2023**, https://doi.org/10.1007/s40011-023-01444-9.
23. Fardood, S.T.; Moradnia, F.; Heidarzadeh, S.; Naghipour, A. Green synthesis, characterization, photocatalytic and antibacterial activities of copper oxide nanoparticles of copper oxide nanoparticles. *Nanochem. Res.* **2023**, *8*, 134-140, https://doi.org/10.22036/ncr.2023.02.006.
24. (~~a~~)Isik, Z.; Bouchareb, R.; Arslan, H.; Özdemir, S.; Gonca, S.; Dizge, N.; Balakrishnan, D.; Prasad, S.V.S. Green synthesis of iron oxide nanoparticles derived from water and methanol extract of *Centaurea solstitialis* leaves and tested for antimicrobial activity and dye decolorization capability. *Env. Res.* **2023**, *219*, 115072, https://doi.org/10.1016/j.envres.2022.115072.
25. Balaba, N.; Jaerger, S.; Horsth, D.F.L.; Primo, J.d.O.; Correa, J.d.S.; Bittencourt, C.; Zanette, C.M.; Anaissi, F.J. Polysaccharides as Green Fuels for the Synthesis of MgO: Characterization and Evaluation of Antimicrobial Activities. *Molecules* **2023**, *28*, 142, https://doi.org/10.3390/molecules28010142.
26. Kavitha, A.; Doss, A.; Pole, R.P.P.; Rani, T.P.K.P.; Prasad, R.; Satheesh, S. A mini review on plant-mediated zinc oxide nanoparticles and their antibacterial potency. *Biocatal. Agric. Biotechnol.* **2023**, *48*, 102654, https://doi.org/10.1016/j.bcab.2023.102654.

27. Carrapiço, A.; Martins, M.R.; Caldeira, A.T.; Mirão, J.; Dias, L. Biosynthesis of Metal and Metal Oxide Nanoparticles Using Microbial Cultures: Mechanisms, Antimicrobial Activity and Applications to Cultural Heritage. *Microorganisms* **2023**, *11*, 378, https://doi.org/10.3390/microorganisms11020378.
28. Samsulkahar, N.F.; Hadi, A.A.; Shamsuddin, M.; Nizam N.A.N.M. Biosynthesis of Gold Nanoparticles Using *Strobilanthes crispa* Aqueous Leaves Extract and Evaluation of Its Antibacterial Activity. *Biointerface Res. Appl. Chem.* **2023**, *13*, 63, https://doi.org/10.33263/BRIAC131.063.
29. Huang, L; Li, D.Q.; Lin, Y.J.; Wei, M.; Evans, D.G.; Duan, X. Controllable preparation of Nano-MgO and investigation of its bactericidal properties. *J. Inorg. Biochem.* **2005**, *99*, 986–993, https://doi.org/10.1016/j.jinorgbio.2004.12.022.
30. Sawai, J.; Kawada, E.; Kanou, F.; Igarashi, H.; Hashimoto, A.; Kakugan, T.; Shimizu, M. Detection of Active Oxygen Generated from Ceramic Powders Having Antibacterial Activity. *J. Chem. Eng. Japan* **1996**, *29*, 627–633, https://doi.org/10.1252/jcej.29.627.
31. Krishnamoorthy, V.; Hiller, D.B.; Ripper, R.; Lin, B.; Vogel, S.M.; Feinstein, D.L.; Oswald, S.; Rothschild, L.; Hensel, P.; Rubinstein, I.; Minshall, R.; Weinberg, G.L. Epinephrine Induces Rapid Deterioration in Pulmonary Oxygen Exchange in Intact, Anesthetized Rats: A Flow and Pulmonary Capillary Pressure-dependent Phenomenon. *Anesthesiology* **2012**, *117*, 745–754, https://doi.org/10.1097/aln.0b013e31826a7da7.
32. Klabunde, K.J. Nanoscale Materials in Chemistry, Klabunde, K.J, Eds.; Wiley-VCH, New York **2001**, 223-26, https://doi.org/10.1002/0471220620.
33. Jin, T.; He, Y. Antibacterial activities of magnesium oxide (MgO) nanoparticles against foodborne pathogens. *J Nanopart Res.* **2011**, *13*, 6877–6885, https://doi.org/10.1007/s11051-011-0595-5.
34. Lai, J.C.K.; Lai, M.B.; Jandhyam, S.; Dukhande, V.V.; Bhushan, A.; Daniels, C.K.; Leung, S.W. Exposure to titanium dioxide and other metallic oxide nanoparticles induces cytotoxicity on human neural cells and fibroblasts. *Int. J. Nanomedicine* **2008**, *3*, 533-545, https://doi.org/10.2147/ijn.s3234.
35. Vidic, J.; Stankic, S.; Haque, F.; Ciric, D.; Le Goffic, R.; Vidy, A.; Jupille, J.; Delmas, B. Selective antibacterial effects of mixed ZnMgO nanoparticles. *J. Nanopart. Res.* **2013**, *15*, 1595, https://doi.org/10.1007/s11051-013-1595-4.
36. Sawai, J.; Kojima, H.; Igarashi, H.; Hashimoto, A.; Shoji, S.; Takehara, A.; Sawaki, T.; Kokugan, T.; Shimizu, M. Escherichia *coli* Damage by Ceramic PowderSslurries. *J. Chem. Eng. Japan* **1997**, *30*, 1034–1039, https://doi.org/10.1252/jcej.30.1034.
37. Lellouche, J.; Kahana, E.; Elias, S.; Gedanken, A.; Banin, E. Antibiofilm activity of nanosized magnesium fluoride. *Biomaterials* **2009**, *30*, 5969-5978, https://doi.org/10.1016/j.biomaterials.2009.07.037.
38. Liu, X.; He, X.; Jin, D.; Wu, S.; Wang, H.; Yin, M.; Aldalbahi, A.; El-Newehy, M.; Mo, X.; Wu, J. A biodegradable multifunctional nanofibrous membrane for periodontal tissue regeneration. *Acta Biomater*, **2020**, *108*, 207–222, https://doi.org/10.1016/j.actbio.2020.03.044.
39. Ababzadeh, S.; Farzin, A.; Goodarzi, A.; Karimi, R.; Farahani, M.S.; Farsani, M.E.; Gharibzad, M.; Zahiri, M.; Ai, J. High porous electrospun poly(ε-caprolactone)/gelatin/MgO scaffolds preseeded with endometrial stem cells promote tissue regeneration in full-thickness skin wounds: An in vivo study. *J. Biomed. Mater. Res., Part B: App. Biomaterials* **2020**, *108*, 2961–2970, https://doi.org/10.1002/jbm.b.34626.
40. Mingyue Liu; Xiaoyu Wang; Haiyan Li; Changlei Xi; Zhengni Liu; Jiajie Liu; Anlin Yin; Xiangxin Lou; Hongsheng Wang; Xiumei Mo; Jinglei Wu. Magnesium oxide-incorporated electrospun membranes inhibit bacterial infections and promote the healing process of infected wounds. *J. Mater. Chem. B* **2021**, 9, 3727, https://doi.org/10.1039/d1tb00217a.
41. He, Y.; Ingudam, S.; Reed, S.; Gehring, A.; Jr. Strobaugh, T.P.; Irwin, P. Study on the mechanism of antibacterial action of magnesium oxide nanoparticles against foodborne pathogens. *J. Nanobiotechnol.* **2016**, *14*, 54, https://doi.org/10.1186/s12951-016-0202-0.
42. Karthik, K.; Dhanuskodi, S.; Gobinath, C.; Prabukumar, S.; Sivaramakrishnan, S. Fabrication of MgO nanostructures and its efficient photocatalytic, antibacterial and anticancer performance. *J. Photochem. Photobiol. B*: *Biology* **2019**, *190*, 8–20, https://doi.org/10.1016/j.jphotobiol.2018.1 001.
43. Kong, F.; Wang, J.; Han, R.; Ji, S.; Yue, J.; Wang, Y.; Ma, L. Antifungal Activity of Magnesium Oxide Nanoparticles: Effect on the Growth and Key Virulence Factors of *Candida albicans*. *Mycopathologia* **2020**, *185*, 485–494, https://doi.org/10.1007/s11046-020-00446-9.
44. Abid, S.; Uzair, B.; Nazi, M.B.K.; Fasim, F.; Bano, S.A.; Jamil, N.; Batool, R.; Sajjad, S. Bursting the Virulence Traits of MDR Strain of *Candida albicans* Using Sodium Alginate-based Microspheres

Containing Nystatin-loaded MgO/ CuO Nanocomposites. *Int. J. Nanomed.* **2021**, *16*, 1157–1174, https://doi.org/10.2147/IJN.S282305.
45. Sharma, G.; Soni, R.; Jasuja, N.D. Phytoassisted synthesis of magnesium oxide nanoparticles with *Swertia chirayaita*. *J. Taibah Univ. Sci.* **2017**, *11*, 471-477, https://doi.org/10.1016/j.jtusci.2016.09.004.
46. Abdel-Aziz, M.M.; Emam, T.M.; Elsherbiny, E.A. Bioactivity of magnesium oxide nanoparticles synthesized from cell filtrate of endobacterium *Burkholderia rinojensis* against *Fusarium oxysporum*. *Mater. Sci. Eng. C.* **2020**, *109*, 110617, https://doi.org/10.1016/j.msec.2019.110617.
47. Depoorter, E.; Bull, M.J.; Peeters, C.; Coenye, T.; Vandamme, P.; Mahenthiralingam, E. *Burkholderia*: an update on taxonomy and biotechnological potential as antibiotic producers. *Appl. Microbiol. Biotechnol.* **2016**, *100*, 5215–5229, https://doi.org/10.1007/s00253-016-7520-x.
48. Esmaeel, Q.; Jacquard, C.; Clément, C.; Sanchez, L.; Barka, E.A. Genome sequencing and traits analysis of *Burkholderia* strains reveal a promising biocontrol effect against grey mould disease in grapevine (*Vitis vinifera* L.). *World J. Microbiol. Biotechnol.* **2019**, *35*, 40, https://doi.org/10.1007/s11274-019-2613-1.
49. Ramanujam, K.; Sundrarajan, M. Antibacterial effects of biosynthesized MgO nanoparticles using ethanolic fruit extract of *Emblica officinalis*. *J. Photochem. Photobiol. B: Biol.* **2014**, *141*, 296-300, https://doi.org/10.1016/j.jphotobiol.2014.09.011.
50. Aničˇić, N.; Vukomanovic, M.; Suvorov, D. The nano-texturing of MgO microrods for antibacterial applications. *RSC Adv.* **2016**, *6*, 102657–102664, https://doi.org/10.1039/C6RA23058J.
51. Anicic, N.; Vukomanovic, M.; Koklicˇ, T.; Suvorov, D. Fewer Defects in the Surface Slows the Hydrolysis Rate, Decreases the ROS Generation Potential, and Improves the Non-ROS Antimicrobial Activity of MgO. *Small* **2018**, *14*, 1800205, https://doi.org/10.1002/smll.201800205.
52. Aničić, N.; Kurtjak, M.; Jeverica, S.; Suvorov, D.; Vukomanovic, M. Antimicrobial Polymeric Composites with Embedded Nanotextured Magnesium Oxide. *Polymers* **2021**, *13*, 2183, https://doi.org/10.3390/polym13132183.
53. Hickey, D.J.; Ercan, B.; Sun, L.; Webster, T.J. Adding MgO nanoparticles to hydroxyapatite-PLLA nanocomposites for improved bone tissue engineering applications. *Acta Biomater.* **2015**, *14*, 175-184, https://doi.org/10.1016/j.actbio.2014.12.004.
54. Diaz, R.M.; Cardoso-Avila, P.E.; Tavares, J.A.P.; Patakfalvi, R.; Cruz, V.V.; Ladrón de Guevara, H.P.; Coronado, O.G.; Garibay, R.I.A.; Arroyo, Q.E.S.; Marañón-Ruiz, V.F.; Contreras, J.C. Two-Step Triethylamine-Based Synthesis of MgO Nanoparticles and Their Antibacterial Effect against Pathogenic Bacteria. *Nanomaterials* **2021**, *11*, 410, https://doi.org/10.3390/nano11020410.
55. Sawai, J.; Kojima, H.; Igarashi, H.; Hashimoto, A.; Shoji, S.; Sawaki, T.; Hakoda, A.; Kawada, E.; Kokugan, T.; Shimizu, M. Antibacterial characteristics of magnesium oxide powder. *World J. Microbiol. Biotechnol.* **2000**, *16*, 187–194, https://doi.org/10.1023/A:1008916209784.
56. Hickey, D.J.; Muthusamy, D.; Webster, T.J. Electrophoretic deposition of MgO nanoparticles imparts antibacterial properties to poly-L-lactic acid for orthopedic applications. *J. Biomed. Mater. Res. Part A* **2017**, *105*, 3136–3147, https://doi.org/10.1002/jbm.a.36174.
57. Han, P.; Cheng, P.; Zhang, S.; Zhao, C.; Ni, J.; Zhang, Y.; Zhong, W.; Hou, P.; Zhang, X.; Zheng, Y.; Chai, Y. *Invitro* and *invivo* studies on the degradation of high-purity Mg (99.99 wt.%) screw with femoral intracondylar fractured rabbit model. *Biomaterials* **2015**, *64*, 57−69, https://doi.org/10.1016/j.biomaterials.2015.06.031.
58. Huang, S.; Wang, B.; Zhang, X.; Lu, F.; Wang, Z.; Tian, S.; Li, D.; Yang, J.; Cao, F.; Cheng, L.; Gao, Z.; Li, Y.; Qin, K., Zhao, D. High-purity weight-bearing magnesium screw: Translational application in the healing of femoral neck fracture. *Biomaterials* **2020**, *238*, 119829, https://doi.org/10.1016/j.biomaterials.2020.119829.
59. Zhao, D.; Huang, S.; Lu, F.; Wang, B.; Yang, L.; Qin, L.; Yang, K.; Li, Y.; Li, W.; Wang, W.; Tian, S.; Zhang, X.; Gao, W.; Wang, Z.; Zhang, Y.; Xie, X.; Wang, J.; Li, J. Vascularized bone grafting fixed by biodegradable magnesium screw for treating osteonecrosis of the femoral head. *Biomaterials* **2016**, *81*, 84−92, https://doi.org/10.1016/j.biomaterials.2015.1 038.
60. Lin, J.; Nguyen, N-Y.T.; Zhang, C.; Ha, A.; Liu, H.H. Antimicrobial Properties of MgO Nanostructures on Magnesium Substrates. *ACS Omega* **2020**, *5*, 24613−24627, https://doi.org/10.1021/acsomega.0c03151.
61. Foyer, C.H.; Lopez-Delgado, H.; Dat, J.F.; Scott, I.M. Hydrogen peroxide- and glutathione-associated mechanisms of acclamatory stress tolerance and signaling. *Physiol. Plant.* **1997**, *100*, 241–254, https://doi.org/10.1111/j.1399-3054.1997.tb04780.x.

62. Robert-Seilaniantz, A.; Grant, M.; Jones, J.D.G. Hormone Crosstalk in Plant Disease and Defense: More Than Just JASMONATE-SALICYLATE Antagonism. *Annu. Rev. Phytopathol.* **2011**, *49*, 317–343. https://doi.org/10.1146/annurev-phyto-073009-114447.
63. Imada, K.; Sakai, S.; Kajihara, H.; Tanaka, S.; Ito, S. Magnesium oxide nanoparticles induce systemic resistance in tomato against bacterial wilt disease. *Plant Pathol.* **2016**, *65*, 551–560, https://doi.org/10.1111/ppa.12443.
64. Chen, J.; Wu, L.; Lu, M.; Lu, S.; Li, Z.; Ding, W. Comparative Study on the Fungicidal Activity of Metallic MgO Nanoparticles and Macroscale MgO Against Soilborne Fungal Phytopathogens. *Front. Microbiol.* **2020**, *11*, 365, https://doi.org/10.3389/fmicb.2020.00365.
65. Ogunyemi, S.O.; Zhang, F.; Abdallah, Y.; Zhang, M.; Wang, Y.; Sun, G.; Qiu, W.; Li, B. Biosynthesis and characterization of magnesium oxide and manganese dioxide nanoparticles using *Matricaria chamomilla* L. extract and its inhibitory effect on *Acidovorax oryzae* strain RS-2. *Artif. Cells, Nanomed., Biotechnol.*, **2019**, *47*, 2230-2239, https://doi.org/10.1080/2169140 2019.1622552.
66. Abdallah, Y.; Ogunyemi, S.O.; Abdelazez, A.; Zhang, M.; Hong, X.; Ibrahim, E.; Hossain, A.; Fouad, H.; Li, B.; Chen, J. The Green Synthesis of MgO Nano-Flowers Using *Rosmarinus officinalis L*. (Rosemary) and the Antibacterial Activities against *Xanthomonas oryzae* pv. *Oryzae*. *BioMed Res. Int.* **2019**, *2019*, 1-8, https://doi.org/10.1155/2019/5620989.
67. Sidhu, A.; Bala, A.; Singh, H.; Ahuja, R.; Kumar, A. Development of MgO-sepoilite Nanocomposites against Phytopathogenic Fungi of Rice (*Oryzae sativa*): A Green Approach. *ACS Omega* **2020**, *5*, 13557−13565, https://doi.org/10.1021/acsomega.0c00008.
68. Cai, L.; Chen, J.; Liu, Z.; Wang, H.; Yang, H.; Ding, W. Magnesium Oxide Nanoparticles: Effective Agricultural Antibacterial Agent Against *Ralstonia solanacearum*. *Front. Microbiol*. **2018**, *9*, 790, https://doi.org/10.3389/fmicb.2018.00790.
69. Panchal, P.; Paul, D.R.; Gautam, S.; Meena, P.; Nehra, S.P.; Maken, S.; Sharma, A. Photocatalytic and antibacterial activities of green synthesized Ag doped MgO nanocomposites towards environmental sustainability. *Chemosphere* **2022**, *297*, 134182, https://doi.org/10.1016/j.chemosphere.2022.134182.
70. Li, X.; Hong, X.; Yang, Y.; Zhao, J.; Diko, C.S.; Zhu, Y. Enhanced antibacterial activity of acid treated MgO nanoparticles on *Escherichia coli*. *RSC Adv*. **2021**, *11*, 38202-38207, https://doi.org/10.1039/D1RA06221B.
71. Wu, Z.; Xu, H.; Xie, W.; Wang, M.; Wang, C.; Gao, G.; Gu, F.; Liu, J.; Fu, J. Study on a novel antibacterial light-cured resin composite containing nano-MgO. *Colloids Surf. B: Biointerfaces* **2020**, *188*, 110774, https://doi.org/10.1016/j.colsurfb.2020.110774.
72. Hong, X.; Yang, Y.; Li, X.; Abitonze, M.; Diko, C.S.; Zhao, J.; Ma, Q.; Liu, W.; Zhu, Y. Enhanced anti-*Escherichia coli* properties of Fe-doping in MgO nanoparticles. *RSC Adv*. **2021**, *11*, 2892-2897, https://doi.org/10.1039/D0RA09590G.
73. Rao, Y.; Wang, W.; Tan, F.; Cai, Y.; Lu, J.; Qiao, X. Influence of different ion doping on antibacterial properties of MgO. *Appl. Surf. Sci*. **2013**, *284*, 726–731, https://doi.org/10.1016/j.apsusc.2013.08.001.
74. Lala, N.L.; Ramaseshan, R.; Bojun, L.; Sundarrajan, S.; Barhate, R.S.; Ying-jun, L.; Ramakrishna, S. Fabrication of nanofibers with antimicrobial functionality used as filters: protection against bacterial contaminants. *Biotechnol. Bioeng.* **2007**, *97*, 1357–1365, https://doi.org/10.1002/bit.21351.
75. Almontasser, A.; Parveen, A. Probing the effect of Ni, Co and Fe doping concentrations on the antibacterial behaviors of MgO nanoparticles. *Sci. Rep.* **2022**, *12*, 7922, https://doi.org/10.1038/s41598-022-12081-z.
76. Siaw, Y.M.; Jeevanandam, J.; Hii, Y.S.; Chan, Y.S. Photo-irradiation coupled biosynthesis of magnesium oxide nanoparticles for antibacterial application. *Naunyn-Schmiedeb. Arch. Pharmacol.* **2020**, *393*, 2253–2264, https://doi.org/10.1007/s00210-020-01934-x.
77. Ammulu, M.A.; Viswanath, K.V.; Giduturi, A.K.; Vemuri, P.K.; Mangamuri, U.; Poda, S. Phytoassisted synthesis of magnesium oxide nanoparticles from *Pterocarpus marsupium* rox.b heartwood extract and its biomedical applications. *J. Genet. Eng. Biotechnol.* **2021**, *19*, 21, https://doi.org/10.1186/s43141-021-00119-0.
78. Das, B.; Moumita, S.; Ghosh, S.; Khan, M.I.; Indira, D.; Jayabalan, R.; Tripathy, S.K.; Mishra, A.; Balasubramanian, P. Biosynthesis of magnesium oxide (MgO) nanoflakes by using leaf extract of *Bauhinia purpurea* and evaluation of its antibacterial property against *Staphylococcus aureus*. *Mater. Sci. Eng. C.* **2018**, *91*, 436-444, https://doi.org/10.1016/j.msec.2018.05.059.
79. Hassan, S.E.-D.; Fouda, A.; Saied, E.; Farag, M.M.S.; Eid, A.M.; Barghoth, M.G.; Awad, M.A.; Hamza, M.F.; Awad, M.F. *Rhizopus oryzae*-Mediated Green Synthesis of Magnesium Oxide Nanoparticles (MgO-

NPs): A Promising Tool for Antimicrobial, Mosquitocidal Action, and Tanning Effluent Treatment. *J. Fungi* **2021**, *7*, 372, https://doi.org/10.3390/jof7050372.
80. Fouda, A.; Awad, M.A.; Eid, A.M.; Saied, E.; Barghoth, M.G.; Hamza, M.F.; Awad, M.F.; Abdelbary, S.; Hassan, S.E.-D. An Eco-Friendly Approach to the Control of Pathogenic Microbes and *Anopheles stephensi* Malarial Vector Using Magnesium Oxide Nanoparticles (Mg-NPs) Fabricated by *Penicillium chrysogenum*. *Int. J. Mol. Sci*. **2021**, *22*, 5096, https://doi.org/10.3390/ijms22105096.
81. Fouda, A.; Eid, A.M.; Abdel-Rahman, M.A.; EL-Belely, E.F.; Awad, M.A.; Hassan, S.E.-D.; AL-Faifi, Z.E.; Hamza, M.F. Enhanced Antimicrobial, Cytotoxicity, Larvicidal, and Repellence Activities of Brown Algae, *Cystoseira crinita*-Mediated Green Synthesis of Magnesium Oxide Nanoparticles. *Front. Bioeng. Biotechnol*. **2022**, *10*, 849921, https://doi.org/10.3389/fbioe.2022.849921.
82. Mangalampalli, B.; Dumala, N.; Grover, P. Acute oral toxicity study of magnesium oxide nanoparticles and microparticles in female albino Wistar rats. *Regul. Toxicol. Pharmacol*. **2017**, *90*, 170–184, https://doi.org/10.1016/j.yrtph.2017.09.005.
83. Martinez-Boubeta, C.; Balcells, L.; Cristòfol, R.; Sanfeliu, C.; Rodríguez, E.; Weissleder, R.; Lope-Piedrafita, S.; Simeonidis, K.; Angelakeris, M.; Sandiumenge, F.; Calleja, A.; Cacas, L.; Monty, C.; Martinez, B. Self-Assembled Multifunctional Fe/MgO Nanospheres for Magnetic Resonance Imaging and Hyperthermia. Nanomed.: Nanotechnol. *Biol. Med*. **2010**, *6*, 362–370, https://doi.org/10.1016/j.nano.2009.09.003.
84. Behzadi, E.; Sarsharzadeh, R.; Nouri, M.; Attar, F.; Akhtari, K.; Shahpasand, K.; Falahati, M. Albumin binding and anticancer effect of magnesium oxide nanoparticles. *Int. J. Nanomed.* **2019**, *14*, 257–270, https://doi.org/10.2147/IJN.S186428.
85. Kum, C.H.; Cho, Y.; Seo, S.H.; Joung, Y.K.; Ahn, D.J.; Han, D.K. A Poly(lactide) Stereo complex Structure with Modified Magnesium Oxide and Its Effects in Enhancing the Mechanical Properties and Suppressing Inflammation. *Small* **2014**, *10*, 3783-3794, https://doi.org/10.1002/smll.201302880.
86. Praphakar, R.A.; Jeyaraj, M.; Mehnath, S.; Higuchi, A.; Ponnamma, D.; Sadasivuni, K.K.; Rajan, M. A pH-sensitive guar gum-*grafted*-lysine-β-cyclodextrin drug carrier for the controlled release of 5-flourouracil into cancer cells. *J. Mater. Chem. B* **2018**, *6*, 1519– 1530, https://doi.org/10.1039/C7TB02551C.
87. El-Zeiny, H.M.; Abukhadra, M.R.; Sayed, O.M.; Osman, A.H.M.; Ahmed, S.A. Insight into novel β-cyclodextrin-grafted-poly (N-vinylcaprolactam) nanogel structures as advanced carriers for 5-fluorouracil: Equilibrium behavior and pharmacokinetic modeling. *Colloids Surf. A: Physicochem. Eng. Aspects* **2020**, *586*, 124197, https://doi.org/10.1016/j.colsurfa.2019.124197.
88. Macedo, L.O.; Barbosa, E.J.; Löbenberg, R.; Bou-Chacra, N.A. Anti-inflammatory drug nanocrystals: state of art and regulatory perspective. *Eur. J. Pharmac. Sci*. **2021**, *158*, 105654, https://doi.org/10.1016/j.ejps.2020.105654.
89. Lu, C.; Xiao, Y.; Liu, Y.; Sun, F.; Qiu, Y.; Mu, H.; Duan, J. Hyaluronic acid-based levofloxacin nanomicelles for nitric oxide-triggered drug delivery to treat bacterial infections. *Carbohydr. Polym*. **2020**, *229*, 115479, https://doi.org/10.1016/j.carbpol.2019.115479.
90. Rahbar, M.; Morsali, A.; Bozorgmehr, M.R.; Beyramabadi, S.A. Quantum chemical studies of chitosan nanoparticles as effective drug delivery systems for 5-fluorouracil anticancer drug. *J. Mol. Liq*. **2020**, *302*, 112495, https://doi.org/10.1016/j.molliq.2020.112495.
91. Othman, S.I.; Allam, A.A.; Al Fassam, H.; Abu-Taweel, G.M.; Altoom, N.; Abukhadra, M.R. Sonoco Green Decoration of Clinoptilolite with MgO Nanoparticles as a Potential Carrier for 5-Fluorouracil Drug: Loading Behavior, Release Profile, and Cytotoxicity. *J. Inorg. Organomet. Polym. Mater*. **2021**, *31*, 4608–4622, https://doi.org/10.1007/s10904-021-02078-y.
92. El-Sawy, N.M.; Raafat, A.I.; Badawy, N.A.; Mohamed, A.M. Radiation development of pH-responsive (xanthan-acrylic acid)/MgO nanocomposite hydrogels for controlled delivery of methotrexate anticancer drug. *Int. J. Biol. Macromol.* **2020**, *142*, 254-264, https://doi.org/10.1016/j.ijbiomac.2019.09.097.
93. Ireson, C.R.; Chander, S.K.; Purohit, A.; Perera, S.; Newman, S.P.; Parish, D.; Leese, M.P.; Smith, A.C.; Potter, B.V.L.; Reed, M.J. Pharmacokinetics and efficacy of 2-methoxyoestradiol and 2-methoxyoestradiol-*bis*-sulphamate *in vivo* in rodents. *Br. J. Cancer*. **2004**, *90*, 932–937, https://doi.org/10.1038/sj.bjc.6601591.
94. Verenich, S.; Gerk, P.M. Therapeutic Promises of 2-Methoxyestradiol and Its Drug Disposition Challenges. *Mol Pharmaceutics.* **2010**, *7*, 2030–2039, https://doi.org/10.1021/mp100190f.
95. Alfaro, A.; Leon, A.; Guajardo-Correa, E.; Reuquen, P.; Torres, F.; Mery, M.; Segura, R.; Zapata, P.a., Orihuela, P.A. MgO nanoparticles coated with polyethylene glycol as carrier for 2-Methoxyestradiol anticancer drug. *PLoS ONE* **2019**, *14*, e0214900, https://doi.org/10.1371/journal.pone.0214900.

96. Karthikeyan, K.; Moon, J.Y.; Hyun, H.B.; Cho, S.K.; Kim, S.-J. Mechanistic investigation on the toxicity of MgO nanoparticles toward cancer cells. *J. Mater. Chem.* **2012**, *22*, 24610-24617, https://doi.org/10.1039/C2JM35087D.
97. She, J.; Yuan, Z.; Wu, Y.; Chen, J.; Kroll, J. Targeting erythropoietin protects against proteinuria in type 2 diabetic patients and in zebrafish. *Mol. Metab*. **2018**, *8*, 189-202, https://doi.org/10.1016/j.molmet.2017.1006.
98. Sutkovic, J.; Jašarević, A. A review on nanoparticle and protein interaction in biomedical applications. *Period. Eng. Nat. Sci.* **2016**, *4*, https://doi.org/10.21533/pen.v4i2.62.
99. Fayed, B.E.; Tawfik, A.F.; Yassin, A.E.B. Novel erythropoietinloaded nanoparticles with prolonged *in vivo* response. *J. Microencapsul*. **2012**, *29*, 650-656, https://doi.org/10.3109/02652048.2012.680507.
100. Yu M, Wu J, Shi J, Farokhzad OC., Nanotechnology for protein delivery: Overview and perspectives. *Journal of Controlled Release*, **2015**, 240:24–37, https://doi.org/10.1016/j.jconrel.2015.10.012.
101. Sultan, A.R.; Al-Kazazz, F.F.M.; Mohammed, A.H. Impact of Magnesium Oxide Nanoparticles on Erythropoietin Hormone Levels in Sera of Patients with Anemia Accompanied with Diabetic Kidney Disease. *Nano Biomed. Eng*. **2020**, *12*, 232-240, https://doi.org/10.5101/nbe.v12i3.p232-240.
102. Booster, J.L.; Sandwijk, A.V.; Reuter, M.A. Conversion of magnesium fluoride to magnesium hydroxide. *Miner. Eng.* **2003**, *16*, 273-281, https://doi.org/10.1016/S0892-6875(03)00002-5.
103. Mishakov, I.V.; Bedilo, A.F.; Richards, R.M.; Chesnokov, V.V.; Volodin, A.M.; Zaikovskii, V.I.; Buyanov, R.A.; Klabunde, K.J. Nanocrystalline MgO as a Dehydrohalogenation Catalyst. *J. Catal*. **2002**, *206*, 40-48, https://doi.org/10.1006/jcat.2001.3474.
104. The Cytotoxics Handbook. *British Journal of Cancer*, **1991**, 1;64(3):611–2, https://doi.org/10.1038/bjc.1991.364.
105. Nawara, K.; Romiszewski, J.; Kijewska, K.; Szczytko, J.; Twardowski, A.; Mazur, M.; Krysinski, P. Adsorption of Doxorubicin onto Citrate-Stabilized Magnetic Nanoparticles. *J. Phys. Chem. C* **2012**, *116*, 5598-5609, https://doi.org/10.1021/jp2095278.
106. Thirunavukkarasu, S.; Mohana, K.V.; Velautham, S.; Raju, K.; Randhir, K. MgO Nanoparticles for Effective Uptake and Release of Doxorubicin Drug: pH Sensitive Controlled Drug Release. *J. Nanosci. Nanotechnol*. **2016**, *16*, 9421-9431, https://doi.org/10.1166/jnn.2016.12164.
107. Ranathunge, T.A.; Karunaratne, D.G.G.P.; Rajapakse, R.M.G.; Watkins, D.L. Doxorubicin Loaded Magnesium Oxide Nanoflakes as pH Dependent Carriers for Simultaneous Treatment of Cancer and Hypomagnesemia. *Nanomaterials* **2019**, *9*, 208, https://doi.org/10.3390/nano9020208.
108. Weerasuriya, D.R.K.; Wijesinghe, W.P.S.L.; Rajapakse, R.M.G. Encapsulation of anticancer drug copper bis(8-hydroxyquinoline) in hydroxyapatite for pH-sensitive targeted delivery and slow release. *Mater. Sci. Eng. C* **2017**, *71*, 206-213, https://doi.org/10.1016/j.msec.2016.10.010.
109. Kumar, R.; Gokulakrishnan, N.; Kumar, R.; Krishna, V.M.; Saravanan, A.; Supriya, S.; Somanathan, T. Can Be a Bimetal Oxide ZnO MgO Nanoparticles Anticancer Drug Carrier and Deliver? Doxorubicin adsorption/released study. *J. Nanosci. Nanotechnol*. **2015**, *15*, 1543–1553, https://doi.org/10.1166/jnn.2015.8915.
110. Alaizeri, Z.M.; Alhadlaq, H.A.; Aldawood, S.; Akhtar, M.J.; Amer, M.S.; Ahamed, M. Facile Synthesis, Characterization, Photocatalytic Activity, and Cytotoxicity of Ag-Doped MgO Nanoparticles. *Nanomaterials* **2021**, *11*, 2915, https://doi.org/10.3390/nano11112915.
111. Jiang, F.; Lee, C.; Zhang, W.; Jiang, W.; Cao, Z.; Chong, H.B.; Yang, W.; Zhan, S.; Li, J.; Teng, Y.; Li, Z.; Xie, J. Radiodynamic therapy with CsI(na)@MgO nanoparticles and 5-aminolevulinic acid. *J. Nanobiotech.* **2022**, *20*, 330, https://doi.org/10.1186/s12951-022-01537-z.
112. Monzavi, A.; Eshraghi, S.; Hashemian, R.; Momen-Heravi, F. In vitro and ex vivo antimicrobial efficacy of nano-MgO in the elimination of endodontic pathogens. *Clin. Oral Invest.* **2015**, *19*, 349–356, https://doi.org/10.1007/s00784-014-1253-y.
113. ~~(a)~~ Srinivasa, C.; Kumar, S.R.S.; Pradeep, S.; Prasad, S.K.; Veerapur, R.; Ansari, M.A.; Alomary, M.N.; Alghamdi, S.; Almehmadi, M.; GC., K.; Daphedar, A.B.; Kakkalameli, S.B.; Shivamallu, C.; Kollur, S.P. Eco-Friendly Synthesis of MnO_2 Nanorods Using *Gmelina arborea* Fruit Extract and Its Anticancer Potency Against MCF-7 Breast Cancer Cell Line. *Int. J. Nanomed.* **2022**, *17*, 901-907, https://doi.org/10.2147/IJN.S335848.
114. Yokel, R.A.; McNamara, P.J. Aluminium toxicokinetics: An updated minireview. *Pharmacol Toxicol* **2001**, *88*, 159-167.

115. Atri, A.; Sherman, S.; Norman, K.A.;Kirchhoff, B.A.; Nicolas, M.M.; Greicius, M.D.; Cramer, S.C.; Breiter, H.C.; Hasselmo, M.E.; Stern, C.E. Blockade of Central Cholinergic Receptors Impairs New Learning and Increases Proactive Interference in a Word Paired-Associate Memory Task. *Behav Neurosci* **2004**, *118*, 223-236, https://doi.org/10.1037/0735-7044.118. 223.
116. Ringman, J.M.; Frautschy, S.A.; Cole, G.M.; Masterman, D.L.; Cummings, J.L. A Potential Role of the Curry Spice Curcumin in Alzheimers Disease. *Curr. Alzheimer Res.* **2005**, *2*, 131-136, https://doi.org/10.2174/1567205053585882.
117. Pan, R.; Qiu, S.; Lu, D.X.; Dong, J. Curcumin improves learning and memory ability and its neuroprotective mechanism in mice. *Chin. Med. J.* **2008**, *121*, 832-839, https://doi.org/10.1097/00029330-200805010-00015.
118. Mignani, S.; El Kazzouli, S.; Bousmina, M.; Majoral. J.P. Expand classical drug administration ways by emerging routes using dendrimer drug delivery systems: A concise overview. *Adv. Drug Deliv. Rev.* **2013**, *65*, 1316-1330, https://doi.org/10.1016/j.addr.2013.0 001.
119. Arora, S.; Rajwade, J.M.; Paknikar, K.M. Nanotoxicology and *in vitro* studies: The need of the hour. *Toxicol. Appl. Pharmacol.* **2012**, *258*, 151-165, https://doi.org/10.1016/j.taap.201 1 010.
120. Fukui, H.; Horie, M.; Endoh, S.; Kato, H.; Fujita, K.; Nishio, K.; Komaba, L.K.; Maru, J.; Miyauhi, A.; Nakamura, A.; Kinugasa, S.; Yoshida, Y.; Hahihara, Y.; Iwahashi, H. Association of zinc ion release and oxidative stress induced by intratracheal instillation of ZnO nanoparticles to rat lung. *Chem. Biol. Interact.* **2012**, *198*, 29-37, https://doi.org/10.1016/j.cbi.2012.04.007.
121. Chalkidou, A.; Simeonidis, K.; Angelakeris, M.; Samaras, T.; Martinez-Boubeta, C.; Balcells, L.; Papazisis, K.; Dendrinou-Samara, C.; Kalogirou, O. *In vitro* application of Fe/MgO nanoparticles as magnetically mediated hyperthermia agents for cancer treatment. *J. Magn. Magn. Mater.* **2011**, *323*, 775-780, https://doi.org/10.1016/j.jmmm.2010.10.043.
122. Moeini-Nodeh, S.; Rahimifard, M.; Baeeri, M.; Abdollahi, M. Functional Improvement in Rats' Pancreatic Islets Using Magnesium Oxide Nanoparticles Through Antiapoptotic and Antioxidant Pathways. *Biol. Trace Elem. Res.* **2017**, *175*, 146-155, https://doi.org/10.1007/s12011-016-0754-8.
123. Süzer, T.; Coskun, E.; Islekel, H.; Tahta, K. Neuroprotective effect of magnesium on lipid peroxidation and axonal function after experimental spinal cord injury. *Spinal Cord* **1999**, *37*, 480-484, https://doi.org/10.1038/sj.sc.3100874.
124. Ganna, S.; Gutturu, R.R.; Megala, R.; Nadella, R.; Borelli, D.P.R.; Nannepaga, J.S. Targeted Delivery of Curcumin Using MgONPs and Solid Lipid Nanoparticles: Attenuates Aluminum-Induced Neurotoxicity in Albino Rats. *Pharmacognosy Res.* **2020**, *12*, 380-386, https://doi.org/10.4103/pr.pr_18_20.
125. Dimitriou, R.; Jones, E.; McGonagle, D.; Giannoudis, P.V. Bone regeneration: current concepts and future directions. *BMC Med.* **2011**, *9*, 66, https://doi.org/10.1186/1741-7015-9-66.
126. Geiger, M.; Li, R.H.; Friess, W. Collagen sponges for bone regeneration with rhBMP-2. *Adv. Drug Deliv. Rev.* **2003**, *55*, 1613-1629, https://doi.org/10.1016/j.addr.2003.08.010.
127. Kim, H.K.W.; Oxendine, I.; Kamiya, N. High-concentration of BMP2 reduces cell proliferation and increases apoptosis via DKK1 and SOST in human primary periosteal cells. *Bone*. **2013**, *54*, 141-150, https://doi.org/10.1016/j.bone.2013.0 031.
128. Giusti, A. Hamdy, N.A.; Dekkers, O.M.; Ramautar, S.R.; Dijkstra, S.; Papapoulos, S.E. Atypical fractures and bisphosphonate therapy: A cohort study of patients with femoral fracture with radiographic adjudication of fracture site and features. *Bone*. **2011**, *48*, 966-977, https://doi.org/10.1016/j.bone.2010.12.033.
129. Park, J.W.; Kim, Y.J.; Jang, J.H.; Song, H. Osteoblast response to magnesium ion-incorporated nanoporous titanium oxide surfaces. *Clin. Oral Implants Res.* **2010,** *21*, 1278-1287, https://doi.org/10.1111/j.1600-050 2010.01944.x.
130. Chatzipanagis, K.; Baumann, C.G.; Sandri, M.; Sprio, S.; Tampieri, A.; Kröger, R. *In situ* mechanical and molecular investigations of collagen/apatite biomimetic composites combining Raman spectroscopy and stress-strain analysis. *Acta Biomater*. **2016**, *46*, 278-285, https://doi.org/10.1016/j.actbio.2016.09.028.
131. Navarro-González, J.F.; Mora-Fernández, C.; García-Pérez, J. *Reviews:* Clinical Implications of Disordered Magnesium Homeostasis in Chronic Renal Failure and Dialysis. *Semin. Dial.* **2009**, *22*, 37-44, https://doi.org/10.1111/j.1525-139X.2008.00530.x.
132. Dong, H.; Li, Q.; Tan, C.; Bai, N.; Cai, P. Bi-directional controlled release of ibuprofen and Mg^{2+} from magnesium alloys coated by multifunctional composite. *Mat. Sci. Eng.: C*. **2016**, *68*, 512-518, https://doi.org/10.1016/j.msec.2016.06.035.

133. Lin, Z.; Wu, J.; Qiao, W.; Zhao, Y.; Wong, K.H.M.; Chu, P.K.; Bian, L.; Wu, S.; Zheng, Y.; Cheung, K.M.C.; Leung, F.; Yeung, K.W.K. Precisely controlled delivery of magnesium ions thru sponge-like monodisperse PLGA/nano-MgO-alginate core-shell microsphere device to enable *in situ* bone regeneration. *Biomater.* **2018**, *174*, 1-16, https://doi.org/10.1016/j.biomaterials.2018.05.011.
134. Rahman, S.; Bhattarai, N. Magnesium Oxide Based PLGA/Chitosan Microparticles for Controlled Release Study. *Int. Mech. Eng. Congr. Expo.* **2015,** *57571*, 1-4, https://doi.org/10.1115/IMECE2015-52143.
135. Amaral, L.F.; Oliveira, I.R.; Salomão, R.; Frollini, E.; Pandolfelli, V.C. Temperature and common-ion effect on magnesium oxide (MgO) hydration. *Ceram. Int.* **2010**, *36*, 1047–1054, https://doi.org/10.1016/j.ceramint.2009.12.009.
136. Shuai, C.; Zan, J.; Qi, F.; Wang, G.; Liu, Z.; Yang, Y.; Peng, S. nMgO-incorporated PLLA bone scaffolds: Enhanced crystallinity and neutralized acidic products. *Mater. Des.* **2019**, *174*, 107801, https://doi.org/10.1016/j.matdes.2019.107801.
137. Niknam, Z.; Golchin, A.; Rezaei–Tavirani, M.; Ranjbarvan, P.; Zali, H.; Omidi, M.; Mansouri, V. Osteogenic Differentiation Potential of Adipose-Derived Mesenchymal Stem Cells Cultured on Magnesium Oxide/Polycaprolactone Nanofibrous Scaffolds for Improving Bone Tissue Reconstruction. *Adv Pharm. Bull.* **2022**, *12*, 142-154, https://doi.org/10.34172/apb.2022.015.
138. He, L.; Liu, X.; Rudd, C. Additive-Manufactured Gyroid Scaffolds of Magnesium Oxide, Phosphate Glass Fiber and Polylactic Acid Composite for Bone Tissue Engineering. *Polymers* **2021**, *13*, 270, https://doi.org/10.3390/polym13020270.
139. Canales, D.A.; Reyes, F.; Saavedra, M.; Peponi, L.; Leonés, A.; Palza, H.; Boccaccini, A.R.; Grünewald, A.; Zapata, P.A. Electrospun fibers of poly (lactic acid) containing bioactive glass and magnesium oxide nanoparticles for bone tissue regeneration. *Int. J. Biol. Macromol.* **2022**, *210*, 324-336, https://doi.org/10.1016/j.ijbiomac.2022.05.047.
140. Liu, P.; Yu, H.; Sun, Y.; Zhu, M.; Duan, Y. A mPEG-PLGA-*b*-PLL copolymer carrier for adriamycin and siRNA delivery. *Biomater.* **2012**, *33*, 4403–4412, https://doi.org/10.1016/j.biomaterials.2012.02.041.
141. Huang, Y.; Zhang, L.; Yang, J.; Zhang, X.; Xu, M. Structure and Properties of Cellulose Films Reinforced by Chitin Whiskers. *Macromol. Mater. Eng.* **2012**, *298*, 303–310, https://doi.org/10.1002/mame.201200011.
142. Liu, W.; Zou, Z.; Zhou, L.; Liu, H.; Wen, W.; Zhou, C.; Luo, B. Synergistic effect of functionalized poly($_L$-lactide) with surface-modified MgO and chitin whiskers on osteogenesis in vivo and in vitro. *Mat. Sci. Eng. C* **2019**, *103*, 109851, https://doi.org/10.1016/j.msec.2019.109851.
143. Liang, H.; Zhao, Y.; Yang, J.; Li, X.; Yang, X.; Sasikumar, Y.; Zhou, Z.; Chen, M. Fabrication, Crystalline Behavior, Mechanical Property and In-Vivo Degradation of Poly(l–lactide) (PLLA)–Magnesium Oxide Whiskers (MgO) Nano Composites Prepared by *In situ* Polymerization. *Polymers* **2019**, *11*, 1123, https://doi.org/10.3390/polym11071123.
144. Ma, F.; Lu, X.; Wang, Z.; Sun, Z.; Zhang, F.; Zheng, Y. Nanocomposites of poly ($_L$-lactide) and surface modified magnesia nanoparticles: Fabrication, mechanical property and biodegradability. *J. Phys. Chem. Solids* **2011**, *72*, 111–116, https://doi.org/10.1016/j.jpcs.2010.1 008.
145. Wen, W.; Liu, K.; Zou, Z.; Zhou, C.; Luo, B. Synergistic Effect of Surface-Modified MgO and Chitin Whiskers on the Hydrolytic Degradation Behavior of Injection Molding Poly ($_L$-lactic acid). *ACS Biomater. Sci. Eng.* **2019**, *5*, 2942−2952, https://doi.org/10.1021/acsbiomaterials.8b01629.
146. Wang, L.; Jia, X.; Chen, Y.; Che, Y.; Yuan, Z. Synthesis, degradability, and cell affinity of poly (DL-lactide-*co*-RS-hydroxyethyl-β-malolactonate). *J. Biomed. Mater. Res. A.* **2008**, *87A*, 459-469, https://doi.org/10.1002/jbm.a.31747.
147. He, B.; Poon, Y.F.; Feng, J.; Chan-Park, M.B. Synthesis and characterization of functionalized biodegradable poly(DL-lactide-*co*-RS-**β**-malic acid). *J. biomed. Mat. Res. A* **2008**, 87A, 254–263, https://doi.org/10.1002/jbm.a.31793.
148. Yang, J.; Cao, X.; Zhao, Y.; Wang, L.; Liu, B.; Jia, J.; Liang, H.; Chen, M. Enhanced pH stability, cell viability and reduced degradation rate of poly(L-lactide)-based composite *in vitro*: effect of modified magnesium oxide nanoparticles. *J. Biomat. Sci., Polymer Edition* **2017**, *28*, 486-503, https://doi.org/10.1080/09205063.2017.1279534.
149. Suryavanshi, A.; Khanna, K.; Sindhu, K.R.; Bellare, J.; Srivastava, R. Magnesium oxide nanoparticle-loaded polycaprolactone composite electrospun fiber scaffolds for bone–soft tissue engineering applications: *in-vitro* and *in-vivo* evaluation. *Biomed. Mater.* **2017**, *12*, 055011, https://doi.org/10.1088/1748-605X/aa792b.

150. Boakye, M.A.D.; Rijal, N.P.; Adhikari, U.; Bhattarai, N. Fabrication and Characterization of Electrospun PCL-MgO-Keratin-Based Composite Nanofibers for Biomedical Applications. *Materials* **2015**, *8*, 4080–4095, https://doi.org/10.3390/ma8074080.
151. Niknam, Z.; Zali, H.; Mansouri, V.; Tavirani, M.R.; Omidi, M. Morphological and Molecular Analysis of Osteoblasts Differentiated from Mesenchymal Stem Cells in Polycaprolactone/Magnesium Oxide/Graphene Oxide Scaffold. *Int. J. Org. Transplant Med.* **2019**, *10*, 171-182, https://pubmed.ncbi.nlm.nih.gov/33312462/.
152. Roh, H.-S.; Lee, C.-M.; Hwang, Y.-H.; Kook, M.-S.; Yang, S.-W.; Lee, D.; Kim, B.-H. Addition of MgO nanoparticles and plasma surface treatment of three-dimensional printed polycaprolactone/hydroxyapatite scaffolds for improving bone regeneration. *Mater. Sci. Eng.: C* **2016**, *74*, 525-535, http://dx.doi.org/10.1016/j.msec.2016.12.054.
153. Galow, A.M.; Rebl, A.; Koczan, D.; Bonk, S.M.; Baumann, W.; Gimsa, J. Increased osteoblast viability at alkaline pH *in vitro* provides a new perspective on bone regeneration. *Biochem. Biophys. Rep*. **2017**, *10*, 17-25, https://doi.org/10.1016/j.bbrep.2017.02.001.
154. Xu, D.; Xu, Z.; Cheng, L.; Gao, X.; Sun, J.; Chen, L. Improvement of the mechanical properties and osteogenic activity of 3D-printed polylactic acid porous scaffolds by nano-hydroxyapatite and nano-magnesium oxide. *Heliyon*, **2022**, *8*, e09748, https://doi.org/10.1016/j.heliyon.2022.e09748.
155. Zhao, Y.; Liang, H.; Zhang, S.; Qu, S.; Jiang, Y.; Chen, M. Effects of Magnesium Oxide (MgO) Shapes on In Vitro and In Vivo Degradation Behaviors of PLA/MgO Composites in Long Term. *Polymers* **2020**, *12*, 1074, https://doi.org/10.3390/polym12051074.
156. Alshaer, W.; Hillaireau, H.; Fattal, E. Aptamer-guided nanomedicines for anticancer drug delivery. *Adv. Drug Deliv. Rev*. **2018**, *134*, 122–137, https://doi.org/10.1016/j.addr.2018.09.011.
157. Tan, K.X.; Danquah, M.K.; Sidhu, A.; Ongkudon, C.M.; Lau, S.Y. Towards targeted cancer therapy: Aptamer or oncolytic virus?. *Eur. J. Pharmaceut. Sci.* **2016**, *96*, 8–19, https://doi.org/10.1016/j.ejps.2016.08.061.
158. Sundaram, P.; Kurniawan, H.; Byrne, M.E.; Wower, J. Therapeutic RNA aptamers in clinical trials. *Eur. J. Pharmaceut. Sci*. **2013**, *48*, 259–271, https://doi.org/10.1016/j.ejps.2012.10.014.
159. Ghahremani, F.; Kefayat, A.; Shahbazi-Gahrouei, D.; Motaghi, H.; Mehrgardi, M.A.; Haghjooy-Javanmard, S. AS1411 aptamer-targeted gold nanoclusters effect on the enhancement of radiation therapy efficacy in breast tumor-bearing mice. *Nanomedicine* **2018**, *13*, 2563–2578, https://doi.org/10.2217/nnm-2018-0180.
160. Subramanian, N.; Kanwar, J.R.; Athalya, P.K.; Janakiraman, N.; Khetan, V.; Kanwar, R.K.; Eluchuri, S.; Krishnakumar, S. EpCAM aptamer mediated cancer cell specific delivery of EpCAM siRNA using polymeric nanocomplex. *J. Biomed. Sci*. **2015**, *22*, 4, https://doi.org/10.1186/s12929-014-0108-9.
161. He, F.; Wen, N.; Xiao, D.; Yan, J.; Xiong, H.; Cai, S.; Liu, Z.; Liu, Y. Aptamer-Based Targeted Drug Delivery Systems: Current Potential and Challenges. *Curr. Med. Chem*. **2018**, *27*, 2189-2219, https://doi.org/10.2174/0929867325666181008142831.
162. Tan, K.X.; Jeevanandam, J.; Pan, S.; Yon, L.S.; Danquah, M.K. Aptamer-navigated copolymeric drug carrier system for *in vitro* delivery of MgO nanoparticles as insulin resistance reversal drug candidate in Type 2 diabetes. *J. Drug Deliv. Sci. Technol.* **2020**, *57*, 101764, https://doi.org/10.1016/j.jddst.2020.101764.
163. Tan, K.X.; Danquah, M.K.; Sidhu. A.; Lau, S.Y.; Ongkudon, C.M. Biophysical characterization of layer-by-layer synthesis of aptamer-drug microparticles for enhanced cell targeting. *Biotechnol. Prog*. **2018**, *34*, 249–261, https://doi.org/10.1002/btpr.2524.